°Master of Technology

Transient Numerical Analysis of Chilldown Phenomena in a LN_2 Transfer Line

Chamarthi Bharat Surya

Department of Mechanical Engineering
National Institute of Technology Rourkela

Transient Numerical Analysis of Chilldown Phenomena in a LN_2 Transfer Line

Thesis submitted in partial fulfillment

of the requirements for the degree of

Master of Technology

in

Mechanical Engineering

(*Specialization*: *Cryogenics & Vacuum technology*)

by

Chamarthi Bharat Surya

(Roll Number: 219ME5406)

based on research carried out

under the supervision of

Dr. Suman Ghosh

May, 2021

Department of Mechanical Engineering

National Institute of Technology Rourkela

Department of Mechanical Engineering
National Institute of Technology Rourkela

May 28, 2021

Certificate of Examination

Roll Number: *219ME5406*
Name: *Chamarthi Bharat Surya*
Title of Dissertation: *Transient Numerical Analysis of Chilldown Phenomena in a LN_2 Transfer Line*

We the below signed, after checking the thesis mentioned above and the official record book (s) of the student, hereby state our approval of the thesis submitted in partial fulfillment of the requirements of the degree of in *Mechanical Engineering* at *National Institute of Technology Rourkela*. We are satisfied with the volume, quality, correctness, and originality of the work.

Dr. Suman Ghosh
Principal Supervisor

Department of Mechanical Engineering
National Institute of Technology Rourkela

Dr. Suman Ghosh
Assistant Professor

May 28, 2021

Supervisor's Certificate

This is to certify that the work presented in the thesis entitled *Transient Numerical Analysis of Chilldown Phenomena in a LN_2 Transfer Line* submitted by *Chamarthi Bharat Surya*, Roll Number 219ME5406, is a record of original research carried out by him under my supervision and guidance in partial fulfillment of the requirements of the degree of Master of technology in *Mechanical Engineering*. Neither this thesis nor any part of it has been submitted earlier for any degree or diploma to any institute or university in India or abroad.

_____

Dr. Suman Ghosh

Dedicated to the Noble folk of Scientific Community

Declaration of Originality

I, *Chamarthi Bharat Surya*, Roll Number *219ME5406* hereby declare that this thesis entitled *Transient Numerical Analysis of Chilldown Phenomena in a LN_2 Transfer Line* presents my original work carried out as a postgraduate student of NIT Rourkela and, to the best of my knowledge, contains no material previously published or written by another person, nor any material presented by me for the award of any degree or diploma of NIT Rourkela or any other institution. Any contribution made to this research by others, with whom I have worked at NIT Rourkela or elsewhere, is explicitly acknowledged in the thesis. Works of other authors cited in this dissertation have been duly acknowledged under the sections "Reference" or "Bibliography".

I am fully aware that in case of any non-compliance detected in future, the Senate of NIT Rourkela may withdraw the degree awarded to me on the basis of the present thesis.

May 28, 2021
NIT Rourkela

Chamarthi Bharat Surya

Acknowledgment

I would like to express my sincere gratitude towards my supervisor **Dr. Suman Ghosh**, for his excellent guidance and valuable suggestions during the course of the project work. His immense support during the tough times of the pandemic has instilled confidence and belief in carrying out the project work.

I would also like to thank the Data Center, NIT Rourkela for providing the High Performance Computing facility which has helped in accomplishing majority of my work.

It goes without saying that the past year has been difficult for each one of us.In spite of these challenging times,the administration of NIT Rourkela has facilitated a safe stay after returning to the institute and I cannot thank them enough.

I would like to thank all the staff and faculty members of the Mechanical Engineering Department for their support during my stay at NIT Rourkela.

May 28, 2021
NIT Rourkela

Chamarthi Bharat Surya
Roll Number: 219ME5406

Abstract

Handling and storage of cryogenic fluids is a crucial step in efficient performance of any cryogenic system. Their relatively low boiling point means frequent phase change when in contact with ambient conditions. If not stored and transferred properly, it may be lead to unpleasant consequences.Chilldown is the first stage in transportation of cryogen. It involves two phase flow arising due to of phase change during boiling of the flowing cryogen. High pressure fluctuations leading to back flow during transportation.

The objective of present work is to numerically investigate the chilldown process in a transfer line and study the variation of various hydrodynamic properties such as pressure, temperature, velocity, volume fraction at different axial locations along the transfer line with time. The transfer line is initially at 300K with liquid nitrogen at 77K flowing through it. Because of extreme temperature difference, boiling and phase change of cryogen takes place with simultaneous drop in transfer line temperature. The outer wall of line is subjected to constant heat flux. Three different cross section planes along the transfer line are considered and time variation pressure, velocity, temperature and Volume fraction are expressed.

This work is accomplished in ANSYS FLUENT. A finite Volume based VOF model is used for these transient simulations. The mass transfer phenomena during phase change is enabled by the Lee Evaporation-condensation model. k - ϵ model is used to account for turbulence.These simulations are repeated for different Reynolds number at inlet in order to study the significance of flow rate on two-phase flow characteristics. It is found that with increase in flow rate, chilldown of the wall is faster. At a very low mass flux, single phase gaseous convection took place. Owing to buoyancy,gaseous nitrogen accumulated at the top of transfer line. Phase change resulted in high flow velocity of gaseous phase.

***Keywords*: *Cryogenic fluid*; *Chilldown*; *Two-phase flow*; *Volume of fluid (VOF)*; *FVM*; *Volume Fraction*.**

Contents

Nomenclature

α	Volume fraction
μ	Dynamic Viscosity ($Pa.s$)
ρ	Density (kg/m^3)
c_p	Specific heat at constant pressure ($J/kg-K$)
CHF	Critical Heat Flux
d	diameter
G	Mass flux ($kg/m^2.s$)
GN_2	Gaseous Nitrogen
h	Heat Transfer Co-efficient (W/m^2-K)
k	Thermal Conductivity ($W/m-K$)
l	Liquid phase
LN_2	Liquid Nitrogen
Nu	Nusselt number
q	Heat Flux (W/m^2)
r_i	Radius of inner wall
r_o	Radius of outer wall
Re	Reynolds Number
sat	Saturation
v	Vapor phase
f	fluid
w	wall

List of Figures

List of Tables

Chapter 1

Introduction

Cryogenic fluids find its application in many industrial processes such as aerospace, chemical, medical etc.Perhaps , the significant use of cryogenic is in space exploration. Liquid hydrogen (LH_2) was used as rocket fuel initially. However, with advent of alternative fuels and their better performance, it is rarely used as rocket fuel. It is still used in industrial applications like metal processing,semiconductor manufacturing etc. Liquid Oxygen (LOX) is used as an oxidizer in cryogenic engines for propulsion. Liquid nitrogen is extensively used in food processing and medical applications.Besides these, cryogenic systems play an integral role in space cooling of sensors and other sensitive instruments. Hence design of these systems with maximum efficiency is a big challenge.For any of the cryogen systems to work with maximum efficiency, effective handling, storage and transport of cryogenic fluids is of utmost importance. Prior to any operation, the cryogenic fluid is transferred to the system from storage tanks, transfer lines and other auxiliary systems.

While a cryogenic fluid enters a pipe or a line which is initially in thermal equilibrium with the surroundings, boiling of cryogen takes place as a result of excessive temperature difference between pipeline and cryogen.Because of the phase change during boiling, two phase flow occurs in the pipeline. There may be an abrupt increase or decrease of pressure in the pipeline during this phenomena and back-flow of cryogen into the storage vessel thereby resulting in no flow of cryogen from the pipe. This process of boiling and phase change happens until thermal equilibrium is established between pipeline and cryogen. This phenomena is called chilldown and after that a single phase flow of cryogen persists. In order to arrest the heat leaks into the pipeline which is at cryogenic temperatures at this point, thermal insulation is provided.

Prior to any transfer of steady state single phase cryogen, the transfer line has to go through this initial chilldown phenomena until a thermal equilibrium with cryogen is established.Therefore, it can be said that chilldown is the first step in transportation of cryogen. It is very important to understand the two phase flow characteristics during this chilldown period. Unstable pressure and velocity fluctuations, high transient heat transfer rates are encountered during this process. From an engineering and design perspective, chilldown process plays a crucial role in developing more robust and stable cryogenic systems. An attempt has been made to study the two phase flow characteristics during

chilldown process numerically using ANSYS FLUENT. The Volume of fluid model coupled with Lee evaporation condensation model is used for these simulations.

1.1 Two-Phase Flow

Multiphase flow in general sense, is the simultaneous flow of several phases. Two-phase flow is the simplest case of multiphase flow where it involves only two phases.This can be a solid-liquid, liquid-gas flow. The term 'two-phase' indicates that the phases involved are of the same chemical substance. For e.g., flow of steam-water, Liquid-gaseous nitrogen are two phase flows. However when the interacting components are of different chemical substance then the term 'Two-component' flow is more apt. for e.g.; flow of air-water, oil-water.Two component flows involving single phase (liquid-liquid) can also be referred as two phase flows since the mathematics involved is similar.For these cases, one component is termed to be the continuous phase and other as a discontinuous phase. However, this distinction does not affect the physics and hence the term two phase flow is more commonly used for any flow involving two phases or components.

In context of cryogenic flow boiling, two phase flow is a common occurrence considering the temperature ranges of ambient conditions the systems experience.Especially in transfer line the flowing cryogen comes into contact with the wall initially maintained at room temperature.The cryogen experiences a rapid in surge of heat flux resulting in boiling and eventually phase change.This phase change results in a simultaneous flow of liquid and gaseous cryogen (two phase flow) until the wall temperature reduces to cryogenic temperatures.

1.2 Boiling regimes during chilldown

A boiling curve explains the relationship between wall heat flux and wall super-heat.Flow boiling resembles a similar pattern that occurs in pool boiling. However, unlike pool boiling , Cryogenic chilldown process starts from the right as shown in Figure 1.1.These are generally referred as pipe quenching or chilldown experiments.Chilldown process starts at **A** where a sub-cooled/saturated liquid cryogen enters the pipe initially at room temperature.As the wall temperature reduces, it proceeds towards **B**.This constitutes film boiling regime. Point **B** referred as Leidenfrost point / Re wetting point denotes the minimum wall temperature required to initiate film boiling. During this regime, there is excessive wall superheat leading to formation of vapor.The pipe wall is in contact with the vapor for the whole duration. After the Leidenfrost point is reached,liquid starts intermittently coming into contact with the wall. This is generally referred as the quenching front and at point **C**, liquid fully establishes contact with the wall.This period is transition boiling and it is accompanied by large temperature drops and sudden increase in wall heat flux. When liquid comes into total

contact with the wall, maximum heat flux is achieved generally expressed as Critical heat flux (CHF).**(C)**.

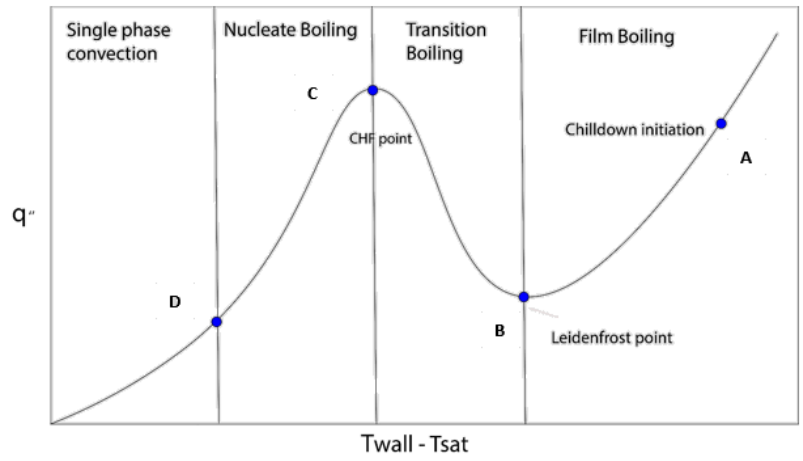

Figure 1.1: Boiling Curve

It can be clearly understood that during film boiling, the presence of low thermal conductivity vapor contact with wall stalled the heat transfer rate thereby resulting in lower heat fluxes whereas presence of quenching front has greatly increased the wall heat flux in transition boiling. Further from C, the wall temperature drops until cryogenic temperatures are reached.

Interpretation of boiling curve can be further enhanced by a chilldown curve. This curve, generally a temperature *vs* time graph shows the wall temperature history through out the chilldown process.

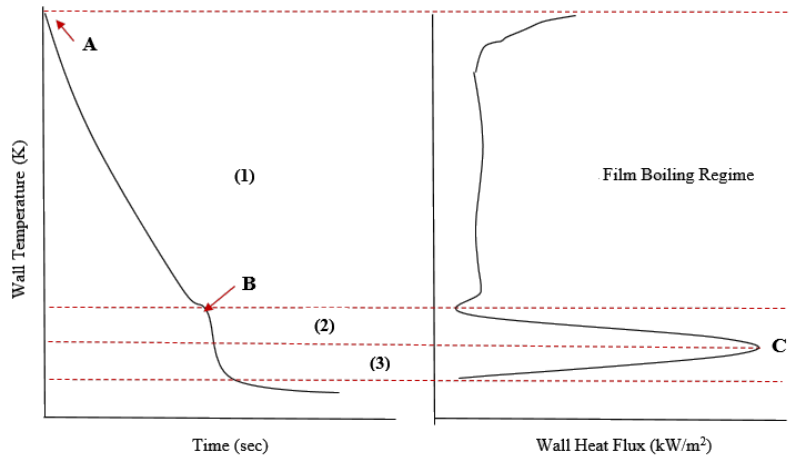

Figure 1.2: Chilldown Curve

It has been established that different boiling regimes are encountered during chilldown.Figure denotes a representative curve of a chilldown phenomena. It can be seen that wall temperature decreases with time at almost a constant rate till the Leidenfrost point **(B)**, after which a sudden drop in observed.This drop is due to the presence of quenching

front which is a characteristic of transition boiling where high heat fluxes from wall to fluid are encountered.As the quenching front propagates the wall temperature decreases along the length. Nucleate boiling exists until a single phase convection of liquid cryogen takes place.A steady flow of liquid cryogen denotes the end of chilldown process. It can be seen that, most of the chilldown process is spent in film boiling regime.

Since liquid cryogen enters an empty transfer line,the upstream section undergoes film boiling.Vapor generated during this event moves downstream undergoing single phase vapor convection.It can be inferred that during this process, different heat transfer regimes coexist along the length. Hence these chilldown curves can be different along the length. Typically upstream sections chilldown faster than downstream sections. These curves also vary with type of fluid, Flow rate, Pressure, Flow orientation with respect to gravity.

During this regime, an annular core of liquid with vapor engulfing it is seen in case of vertical flows.When the wall temperature drops to a certain Leidenfrost temperature, liquid starts coming into contact with the wall and moves ahead which is referred as the quenching front. During this stage regime shifts to transition which is culminated when total liquid comes into contact with the wall. High heat transfer rates and coefficients results in sudden temperature drop of the wall. Heat flux reaches a maximum during the drop and this value is often referred as Critical heat flux (CHF). The temperature drop during this process is such that wall reaches the saturation temperature of cryogen. From there on single phase convection takes place.

Each boiling regime encounters different two phase flow patterns. When the quenching front starts propagating from the upstream, different two phase flow patterns like slug, churn flows are encountered along the transfer line at any given particular instant of time.

1.3 Two-phase flow patterns

Cryogenic line chilldown involves heat transfer from the wall to fluid. Different boiling regimes are encountered during this process.Through visualization experiments, it has been found that flow patterns are characteristic to the boiling regime involved.To make things even more complicated, flow patterns differ along the transfer line.Sequence in which they occur is highly dependent on the geometry and orientation of the transfer line, flow rate, fluid properties, and wall heat flux. It can be implied that the two phase flow patterns greatly effects the heat transfer rate between wall and fluid.

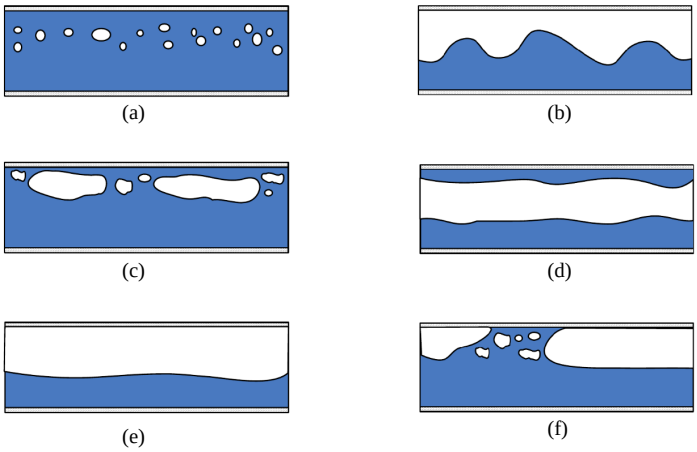

Figure 1.3: Two phase flow patterns
[8]

(a)Bubbly (b)Wavy (c)Slug (d)Annular (e)Stratified (f)Plug

General two phase regimes of air-water mixture have been studied abundantly.The data pertaining to two phase flow during cryogenic boiling is limited and an attempt has been made to summarize the findings.A graphical representation of two phase flow patterns is represented in Figure 1.3. While stratified flow is mostly encountered when the fluids are immiscible, dispersed flow patterns such as plug,bubbly are visible for different oil-water mixture.Annular flow is characteristic to vertical flow boiling and it is even valid in case of cryogenic phase change.

Chapter 2

Literature Survey

Chilldown process involves energy interactions among liquid , gas and the wall.Two phase flow arising as a result of boiling and phase change greatly adds to the complexity of the flow. It is therefore necessary to understand the boiling phenomenon, flow regimes, which will help in gaining a further insight into the heat transfer process.

A comprehensive review of previous research in cryogenic chilldown is done and presented in this chapter

With Space exploration being realized by 1960s, The branch of cryogenics has become a major field of research. Design and optimization of cryogenic systems for space cooling applications was an area of study. Cryogenic fuel handling, storage was a deciding parameter for a cost effective mission. Chilldown phenomena in a cryogenic system was a major research area in cryogenic fuel handling . Initial attempts in studying chill down phenomena dates back to 1960s. Burke *et al.* [1] carried out experiments to study the pressurized cool down of liquid nitrogen lines. Average readings of line temperature, pressure drop, were measured and heat leak into the system was found. An analytical model based on Fourier series was developed to estimate chilldown of concentrated mass.

Efficient transfer of cryogenic propellant to orbit storage tanks is required for accomplishing a successful human space flight. Transfer concepts like chilldown of cryogenic storage tank and chilldown strategies were reviewed by Chato [2] in 1991.A charge-hold-vent technique was used to achieve chilldown with minimum liquid hydrogen consumption.

A computational model of chilldown and propellant loading of the space shuttle external tank was developed using GFSSP program by LeClair [3].This was formulated at NASA's Marshall Space Flight Center.The main objective was to estimate the chilldown time, propellant consumption of entire assembly in order to set a launch time. The simulation results served as validations to a model that predicted upper-stage propellant loading of Ares-1 launch vehicle.

2.1 Experimental studies

Chilldown time of an transfer line is majorly dependent on the geometry, direction of flow with respect to gravity,inlet flow rates,subcooling rates at the inlet. One of the intial chilldown studies were carried out analytically by Srinivasan [4] in the 1970's.Test sections made of glass,Copper,Aluminium and stainless steel were considered. It was deduced that the chilldown time of a short transfer line was independent of inlet flow rate and the dewar pressure.However subsequent experimental studies by Krishnamurthy [5] showed that inlet flow rate greatly affects chilldown times especially in longer transfer lines. Higher flow rated tend to reduce the chilldown time. Also ,presence of multi-layer insulation and vacuum jacketing reduced the chilldown times.

In experiments of chilldown, prediction of heat transfer and heat transfer coefficients of different boiling regimes is an important study. Temperature,Pressure sensors are used to collect data at a high frequency which is then fed to the Data Acquisition systems(DAQ). This data is further processed to obtain relevant heat transfer characteristics and their relation with flow rates,pressure etc. Various Chilldown studies such as the ones that are mentioned in following sections make use of Inverse heat transfer relation proposed by Burggraf [6] to predict inner wall temperature and heat transfer rates. 2.1

$$q''_{i,\text{trans}} = k_t \left[\frac{1}{\alpha_t} \left(\frac{r_i^2 - r_o^2}{2r_i} \right) \frac{\partial T_o}{\partial t} + \frac{1}{4\alpha_t^2} \left(\frac{r_i^3}{4} - \frac{r_0^4}{4r_i} - r_0^2 r_i \ln \frac{r_i}{r_o} \right) \frac{\partial^2 T_0}{\partial t^2} + \frac{1}{32\alpha_t^3} \left(\frac{r_i^5}{12} - \frac{3r_0^4 r_i}{4} + \frac{3r_0^2 r_i^3}{4} - \frac{r_0^6}{12r_i} - r_0^2 r_i^3 \ln \frac{r_i}{r_o} - r_0^4 r_i \ln \frac{r_i}{r_o} \right) \frac{\partial^3 T_o}{\partial t^3} + \cdots \right] \tag{2.1}$$

$q''_{i,\text{trans}}$ is the transient heat flux from wall to the fluid and T_0 is the outer wall temperature which is measured using probes. The temperature history curve, more commonly termed as chilldown curve can be plotted from the obtained data. This plot shows a steady decline in wall temperature followed by a sudden drop, thereby indicating the presence of different boiling regimes during the phenomena.For instance, film boiling regime shifts towards transition and nucleate regimes when Leidenfrost or Rewetting point is reached. heat transfer coefficents drastically change during this shift. Various correlations were emprically proposed which predict the heat transfer coefficients in each boiling regime for a wide set of data.

A comprehensive verification of all existing heat transfer correlations in cryogenic pipe chilldown was put forward by Wang Jiaojiao *et al.* [7]. The study also proposed an accurate chilldown using quasi-steady state method that explain the intricate phase-change and heat transfer dynamics.

2.1.1 Effect of mass flux

S.Darr et al. [8] carried out experiments on a vertical SS304 LN_2 transfer line and studied th effect of various parameters such as mass flux, equilibrium quality, subcooling levels. It was found that the higher the mass flux , the higher the heat transfer rate.This resulted in lower chilldown time. At low mass flux higher equlibrium quality was present at downstream of the line. Varius heat transfer correlations for different boiling regimes were proposed based on these observations.

Jin et al. [9] conducted experiments at low mass flux on a 7m long SS304 LN2 transfer line and monitored the transient histories of temperature, pressure and mass flow rate. Heat transfer characteristics were calculated using the inverse heat transfer problem propsed by Burggraf[6]. This work mainly focused at low mass flux. Oscillations in line pressure and mass flux were observed and particularly were of higher amplitude when system pressures were increased. The Critical heat flux was experimentally found and compared with different available pool boiling correlations.

Since chilldown process is the first step in cryoegnic handling, the primary objective would be to transfer cryogen with minimum consumption and as quickly as possible. high mass flux can cause rapid pressure surges in transfer line leading to back flow of cryogen.Hence, it is important to devise an optimal chilldown strategy specific to each boiling regime for undergoing an efficient chilldown process. Reid Shaeffer [10] embarked upon this problem and proposed a chilldown strategy.A new parameter called chilldown efficiency was defined as the ratio of amount of thermal energy removed from the wall to maximum cooling capability of the cryogen spent in a phase change process.Pulsed flow conditions were tested for its efficiency in carrying out the wall heat.At high Reynolds number in film boiling, these conditions were effective but continuous flow prevailed in other regimes and for other Reynolds number.It was concluded that the overall process is much quicker when continuous flow existed.

Recent Investigations by Hartwig et al .[11] [12] on LH_2 line chilldown showed that the pressure difference between inlet and outlet of the line is a major driver of chilldown process. The effect of pulse and trickle flows was also explored in their studies. Chilldown process was much quicker at high Reynolds number and warm inlet temperatures for trickle flows.

2.1.2 Effect of flow direction with respect to gravity

In a series of studies by S.R.Darr [8] on a liquid nitrogen transfer line of 0.512 m length, emphasis was on estimating the chilldown time for different flow configurations and flow rates. It was observed that when flow was against gravity, chilldown was much quicker. In this case, gravity assists in venting out generated low density vapor. On the other side, Chilldown times were longer for horizontal transfer lines.Circumferential temperature distribution exists at any given section as a result of difference in heat transfer rates at the

bottom and top of transfer line.Due to buoyancy,low thermal conductivity vapor reaches top portions and inhibits the heat transfer rate.Hence, top portions of line take longer time to cooldown eventually contributing to longer chilldown times. Studies were conducted by Johnson [13] on horizontal and inclinded transfer lines of length 2 m and 20 mm inner diameter. Their studies also confirmed the circumferential temperature distribution in horizontal transfer lines , especially at higher flow rates.Transition to nucleate boiling occurred at higher wall temperature due to faster re-flooding of liquid cryogen.Film boiling dominated the bottom part of the wall whereas single phase ga convection existed at the top.Inclination with respect to gravity vector played a major role in chilldown process. Chilldown time reduced as inclination angle was increased with an optimum angle of optimum angle of 10 degrees after which chilldown times started to increase. This effect was more evident at lower mass fluxes. Existence of an optimum inclination angle was also observed in investigations of chilldown by A.K.Shukla [14]. The study also asserts that fluid velocity plays a major role in removing heat from the wall.

2.2 Numerical Studies

Since, cryogenic line chilldown goes through different boiling regimes, heat transfer characteristics vary drastically over time. Hence, separate heat transfer correlations are used for different boiling regimes and two phase flows. A unified model is therefore necessary which can be valid for different flow conditions. Analytical studies in chilldown extensively refine and modify the available correlations which are then used to develop a numerical model.

One of the intial analyical and numerical models were developed by Matthew.F.Cross [15]. A homogeneous two phase flow model using Dittus-Boelter equation for single phase flow and correlations formulated by Miropolskiy [16] were used in chilldown formulation. Also a computer model of Liquid hydrogen line chilldown process using Generalized Fluid System Simulation Program (GFSSP) was simulated.

A 1-D transient numerical chilldown simulation was put forward by S.Darr [17]. Various heat transfer correlations were used to simulate convection heat transfer in each boiling regime. These results were validated by experimental findings of S.Darr et al. [8]. The effect of wall superheat and mass flux on film boiling was studied by Jianye Chen[18]. A 3-D model of vertical LN_2 line was numerically simulated using RPI model coupled with AIAD framework.The drag force existing between liquid and vapor phases was studied. Effect of mass flux on vapor film thickness was investigated as well.

Agarwal [19] worked on the cryogenic two phase flow during phase change and used a sharp interface cut-cell method to model the Inverted Annular film boiling existing at micro-gravity. These chilldown experiments were performed for different cryogens such as Nitrogen,Oxygen,Argon.

FLUENT module of ANSYS was used by Meghna Das Chaudhury [20] to study the characteristics of two phase flow in chilldown process.VOF model coupled with Lee evaporation condensation model was used for these simulations. The effect of flow rate was expressed in terms of area weighted average properties of velocity,pressure,temperature and phase volume fraction.

2.3 Chilldown studies in micro-gravity environment

Cryogenic systems play a major role in space cooling applications.Sensor cooling is achieved using cryogenic fluids and TVS systems maintain sufficient pressure levels by releasing evaporated cryogen. Hence, there have been reduced gravity chilldown studies to predict the two phase flow patterns,heat transfer characteristics. Micro-gravity can be experienced for small instants of time in drop tower tests and aboard parabolic flights of NASA C-9, Boeing KC-135 aircraft.

Chilldown tests were performed aboard the C9 parabolic flight at reduced gravity by Darr *et al.* A SS304 section was considered and chilldown data for upward, downward, horizontal flow configurations was acquired for both 1-g and micro-g conditions. It was seen that for each of the configuration, film boiling Heat transfer rate was 20-25$\%$ lower in reduced gravity. Re-wetting temperatures occurred at much lower at these conditions. In horizontal flow configuration, axisymmetric flow patterns resulted in even cooling of the walls unlike normal 1-g conditions where angular asymmetry in wall temperature existed .However at higher flow rates, these effects diminished. Time averaged heat flux for all configurations were similar in both gravity conditions[21]. While many of the available chilldown studies agree with the findings at higher flow rates, there are some studies which report contrasting results at low flow rates. One such study by Kawamani *et al.* [22] at low flow rates revealed chilldown times were 20$\%$ shorter.Maximum and minimum wall heat fluxes were 1.4 and 1.2 times higher than in the case of terrestrial conditions.

Initial Attempt on flow visualization was done by Antar and Collins [23].Experiments on a 10.5mm I.D, 600mm length quartz tube with saturated liquid nitrogen were carried out aboard the NASA KC-135 aircraft. Also a 4 .32 mm i.d. and 700 mm long SS304 section was used for wall temperature measurements.A new two-phase flow pattern at reduced gravity referred as filamentary flow was introduced for the first time in their observations.It is a sort of inverted annular flow characterized by a long liquid filaments flowing in the center of the channel and surrounded by vapor. These filaments have a diameter of one third of the pipe diameter. Re-wetting time is found to be longer than that at normal gravity. Micro-gravity conditions can only be achieved for small instants of time. Hence, it is extremely difficult to study the two phase flow patterns for entire chilldown phenomena.A study by [24] focused on this aspect and have observed the change reduced gravity makes to the flow patterns. A horizontal Pyrex glass section is subjected to a drop tower test achieving gravity of 10^{-3}g

to 10^{-4} g for 1.7 seconds.Stratified flow which was prevalent in terrestrial conditions.When micro-gravity is experienced,it sent the liquid filaments to the central core and replaced them by low thermal conductivity vapor that significantly reduced the heat transfer from the wall.

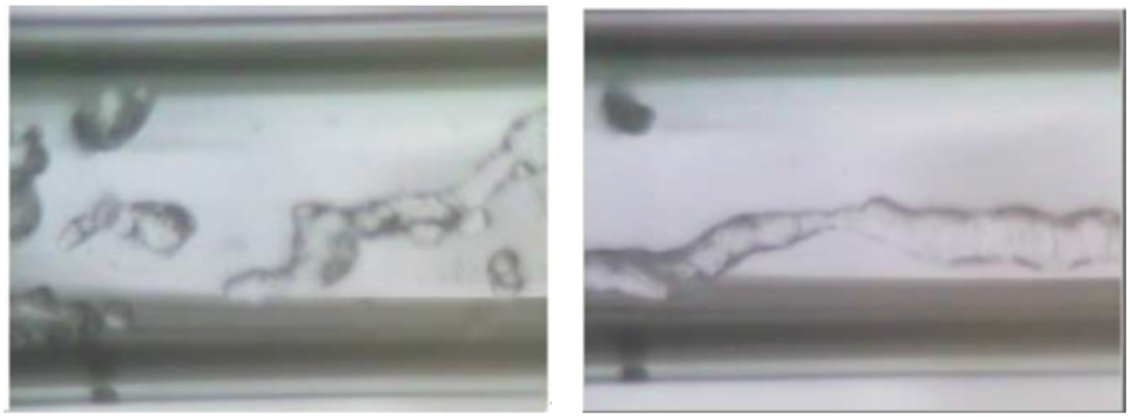

Figure 2.1: Two Phase flow Patterns in Micro-gravity
(a)Low Flow rate (b) High Flow rate [24]

Figure 2.1(a) shows that the effect of reduced gravity resulting in liquid filaments occupying the core.In normal conditions flow is continuous and stratified for higher flow rates.From Figure 2.1(b), reduction in gravity shows that the liquid filaments are lifted up and maintain their shape upon reaching the central core region.

A comprehensive understanding of chilldown phenomena in reduced gravity environment is very much essential for integrating reliant cryogenic systems.Experimental Studies in this area would greatly contribute to making propulsion and space exploration more feasible.

2.4 Concluding remarks

While there is abundant data available for tube heating experiments, cryogenic tube chilldown poses a different challenge.The complex characteristics of heat transfer and two phase flow leads to difficulties in predicting accurate heat transfer phenomena.Parameters like inlet flow rates, sub cooling levels severely affect the heat transfer phenomena.The literature in field of chilldown is abundant but accurate prediction of chilldown phenomena using a unified model that satisfies a wide set of data is still being explored.Various correlations that are characteristics to each boiling regime are being proposed.A well defined two phase flow map of cryogenic chilldown hasn't yet been formulated which makes flow visualization even more necessary. Micro gravity chilldown experiments are simulated in terrestrial conditions which only allow for a few seconds of micro gravity.A complete

study of chilldown, heat transfer and flow visualization studies in the vacuum of space is forthcoming.

The present work primarily focuses on the transient chilldown phenomena of a liquid nitrogen transfer line.Two parts of a problem are numerically simulated using finite volume based VOF method coupled with Lee evaporation-condensation model in ANSYS FLUENT.The first part deals with phase change that occurs as a result of heat leaks into a chilled transfer line.The second part deals with phase change of liquid nitrogen to gaseous nitrogen as a result of chilldown from room temperature. The effect of flow rates is studied and expressed in form of area weighted properties of velocity,temperature,pressure and phase volume fraction.The heat transfer characteristics are then evaluated at different flow rates.

Chapter 3

Methodology

The present work is carried out numerically using the FLUENT module of ANSYS. Transfer line is modeled using the default Design modeler.Inbuilt tool of ANSYS is used to generate a good quality mesh.

3.1 Problem Description

Two independent cases are studied in this work. When the transfer line is initially in thermal equilibrium with surroundings and liquid nitrogen passes through the line,phase change occurs as a result of rapid heat transfer.The then originating complex two phase flow exists until the transfer line reaches cryogenic temperature. The heat transfer characteristics and time variation of several hydrodynamic properties during this phenomena are presented as **Case 1**.

Even though the transfer line reaches cryogenic temperatures , there are heat leaks from the surroundings which might result in boiling and phase change.Such effects are discussed in **Case 2**.

A 1.2 m long, 12 mm ID and 1mm thick stainless steel LN_2 transfer line is considered for the simulations.(Figure 3.1).The gravitational vector is perpendicular to the flow direction thereby making it a horizontal flow configuration. The line is initially maintained at 300K i.e.; thermal equilibrium with the surroundings.Liquid Nitrogen inside the transfer line is at 77K initially.Boiling and phase change takes place in the transfer line as a result of heat

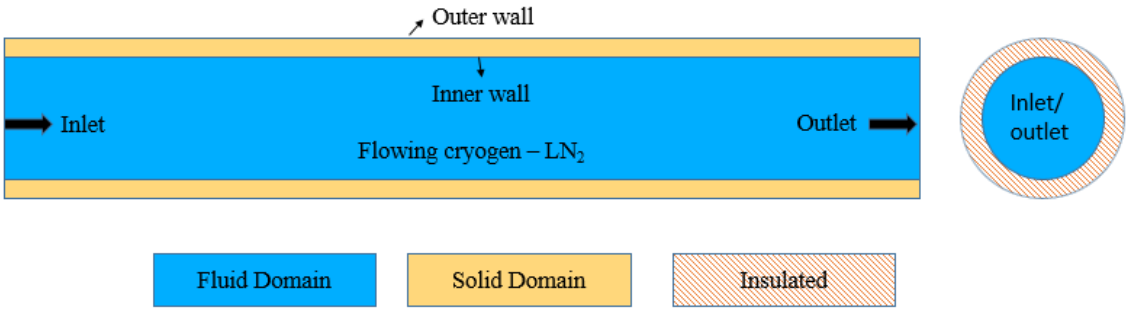

Figure 3.1: Schematic of considered LN_2 Transfer line

transfer. This process is accompanied by drop in wall temperature. Owing to its low density and buoyancy effects, gaseous nitrogen proceeds to accumulate at the top portions while liquid cryogen flows at the bottom portions. Phase change process is a complex phenomena which results in high velocities and pressure surges along the transfer line.Time variation of these hydrodynamic properties are monitored at different cross sections along the transfer line considering various Reynolds number of flow at the inlet. Also, the heat transfer characteristics are expressed in plots of Nusselt number along the length of transfer line

3.2 Objective of the work

- To study the chilldown phenomena in a cryogenic transfer line
- To numerically study the unsteady two phase flow characteristics of cryogen during chilldown of a circular pipe
- To study the two phase flow characteristics in terms of variation of temperature, pressure, volume fraction and velocity in some vertical cross sectional planes with time.Also the spatial distribution of temperature, gas or liquid phase in a particular time instant is studied.
- These studies are repeated for different inlet Reynolds number to capture the effect of inlet flow rates on the flow characteristics.

3.3 3-D Simulation Overview

A full 3-dimensional model is adopted for the transient simulations. ANSYS FLUENT is used to solve the problem numerically. Mesh is checked for its grid independence before proceeding to the simulations. For Case 1, both solid and fluid domains are considered so that drop in temperature of the wall can be studied. For simulations involving Case 2 , only the fluid domain is modeled as it is assumed that the wall is already at cryogenic temperatures and parasitic heat leaks into the system originate from th inner wall. Figure 3.1 shows a schematic of the transfer line in 2-D representing the domains and boundaries involved.

3.3.1 Governing Equations

A finite volume based Volume of Fluid (VOF) model is employed to study the two phase flow characteristics in these simulation.Pressure bases segregated solver is used and gaseous nitrogen phase is assumed to be an ideal gas. The mass interaction between the liquid and vapor phase during phase change (evaporation and condensation) is taken into account by employing Lee evaporation-condensation model coupled with VOF model.

Volume of Fluid method [25] :

Volume of Fluid , generally known as VOF model is a Euler-Euler Approach used for two or more immiscible fluids when their interface is of utmost importance. The concept of phase volume fraction is introduced to measure the presence of a given phase in a cell. The phase volume fraction is represented by α. This method is generally used for stratified flows and slug flows.[25] It can only be used when the dispersion of phases doesn't exist in the flow field.

$$\frac{\partial}{\partial t}\left(\alpha_v \rho_v\right) + \nabla \cdot \left(\alpha_v \rho_v \vec{v_v}\right) = S_\alpha + \left(\dot{\mathbf{m}}_{\mathrm{lv}} - \dot{\mathbf{m}}_{\mathrm{vl}}\right) \tag{3.1}$$

In regard to this problem where liquid and vapor simultaneously exist, the volume fraction/continuity (VF) equation is solved for the vapor phase. α_v , α_l are the volume fractions of vapor and liquid phase respectively. The rates of mass transfer from the equation rae calculated by evaporation and condensation model. S_α is the mass source term for vapor phase. Since $\alpha_l + \alpha_v$ = 1, the liquid volume fraction can be computed if vapor volume fraction is obtained by solving continuity equation. Throughout the computational domain, a single set of momentum equations will be solved and the resultant velocity field is shared among the constituent phases.

$$\frac{\partial}{\partial t}(\rho \bar{v}) + \nabla \cdot (\rho \overline{v}\overline{v}) = -\nabla p + \nabla \cdot \left[\mu \left(\nabla \bar{v} + \nabla \bar{v}^T\right)\right] + \rho \vec{g} + \vec{F} \tag{3.2}$$

Properties ρ and μ are taken as the volume fraction weighted properties of both the phases. **F** represents the external body forces. Volume fraction (α) weighted properties can be expressed as:

$$\rho = \rho_v \times \alpha_v + (1 - \alpha_v) \times \alpha_l \tag{3.3}$$

Mixture density is a combined estimate of densities and volume fraction of phases present in the cell control volume. Similarly, the energy equation is also solved for the present cases and has also been shared among the phases

$$\frac{\partial}{\partial t}(\rho E) + \nabla \cdot (\bar{v}(\rho E + p)) = \nabla \cdot (k \nabla T) + S \tag{3.4}$$

The above equation is deduced from first law of thermodynamics applied to a control volume.S represents various source terms in the form of radiation and from the presence of any chemical reactions.$\nabla \cdot (k \nabla T)$ represents the heat flux due to conduction at the boundary. The left hand side represents the change in energy $E = h - (P/\rho) + (V^2/2)$ of the control volume aided by any external work done. E and T are treated as mass averaged variables for each phase. To account for the turbulence interactions , $k - \epsilon$ model is considered with standard wall functions. Hence two additional transport equations are solved as well.

The value of α in a control volume can only be $0 \leq \alpha \leq 1$. Values of 0 and 1 specify complete existence of either of the phases whereas intermediate values specify the interface between those phases.

Lee evaporation-condensation model

The mass transfer during evaporation is governed in lee model by Vapor Fraction equation (3.1). Positive mass transfer is specified as being from liquid to vapor state.[25]

The amount of mass transferred is calculated using the following equations.
If $T_l > T_{sat}$; Evaporation takes place and

$$\dot{m}_{lv} = f_e \times \alpha_l \rho_l \frac{(T_l - T_{sat})}{T_{\text{sat}}} \tag{3.5}$$

If $T_v < T_{sat}$; Condensation takes place and

$$\dot{m}_{vl} = f_c \times \alpha_v \rho_v \frac{(T_v - T_{sat})}{T_{\text{sat}}} \tag{3.6}$$

here $\dot{m}_{lv}$ and $\dot{m}_{vl}$ are mass transfer during evaporation and condensation respectively. α is volume fraction and ρ is the density. l and v represent liquid and vapor phase respectively.

The coefficients f_e and f_c are referred as evaporation and condensation frequencies on which amount of mass transfer taking place depends. These values are obtained experimentally and often vary during the course of experiment. FLUENT, by default sets these values to $0.1/s$

The afore mentioned governing equations of continuity,momentum,energy and other scalar transport equations are solved iteratively and at each step the values of pressure and velocity are updated such that they satisfy all the involved equations ,thereby attaining convergence.The pressure -velocity coupling is done by using PISO (Pressure Implicit Splitting of Operators). PISO algorithm has an advantage of attaining faster convergence than other segregated solvers like SIMPLE and SIMPLEC. Moreover, this algorithm is preferred for transient simulations and also offers better stability at larger time steps.

Since Fluent is a FVM based tool, the scalar values are designated at the control volume / cell centers. In order to compute the face values , various discretization schemes are used. These are often referred as up-winding schemes FLUENT by default enables available schemes for considered model.However, for more accuracy and better reliability, these can be modified.various discretization schemes used are tabulated in Table 3.1

Pressure at the cell faces is calculated using the Pressure Staggering Option or commonly known as PRESTO.VOF method only allows for PRESTO scheme and body force weighted schemes.Hence, the default option is enabled.For momentum and energy, second order upwinding scheme would give better accuracy with a compromise in computational time.The gradient across the control volume is calculated using Least Squares Cell based which compares itself to be more accurate and less computationally expensive than a node based formulation.

Interface tracking is a crucial part of multiphase flows and Modified High Resolution Interface Capture (Modified-HRIC) technique is used since upwind schemes are numerically diffusive,especially when phase change happens.

Variable	Spatial Discretization Scheme
Pressure	PRESTO
Momentum	Second Order Upwind
Energy	Second Order Upwind
Gradient	Least Squares Cell based
Volume Fraction	Modified HRIC
Turbulent Kinetic energy	First Order Upwind
Dissipation rate	First Order Upwind

Table 3.1: Discretization Schemes used for the simulations

Transient formulation is done using First order implicit scheme as it is the only method available for explicit VOF based solvers.A time step size of 0.001 seconds is used and maximum number of iterations for each time step is set at 70. Convergence of 10^{-6} is set for Momentum,Energy,Turbulent kinetic energy and Dissipation rate. For continuity, a 10^{-4} value of convergence is used.

3.3.2 Material Properties

At low temperatures, the conductivity and specific heat of stainless-steel decrease.From Figure 3.2,It can be seen that these properties decrease by more than 50% at cryogenic temperatures. Hence, this variation is taken into account for the simulations. The variation of specific heat and thermal conductivity of Stainless Steel 304 in the range of 4-300K is given by Marquardt [26] as:

$$\begin{aligned}\log(k) =& a + b\log T + c(\log T)^2 + d(\log T)^3 + e(\log T)^4 + \\ & f(\log T)^5 + g(\log T)^6 + h(\log T)^7 + i(\log T)^8\end{aligned} \tag{3.7}$$

The value of constants differ for specific heat (Cp)and Thermal Conductivity (k).

In order to reduce the computational effort, a regression analysis is used to fit the data within the working range into a polynomial expression. Thereby resulting relations are:

$$\mathbf{c_p}(J/kg-K) = -3\times10^{-7}T^4 + 0.0002T^3 - 0.0748T^2 + 11.382T\text{–}327.84 \tag{3.8}$$

$$\mathbf{k}(W/m-K) = 3.967 + 0.057T\text{–}(7\times10^{-5}T^2) \tag{3.9}$$

Gaseous nitrogen is assumed to be an ideal gas as its compressibiltiy factor in the range of 77K -300K and at atmospheric pressure is nearer to 1. However, at low temperatures and higher pressures, this effect ceases to exist.

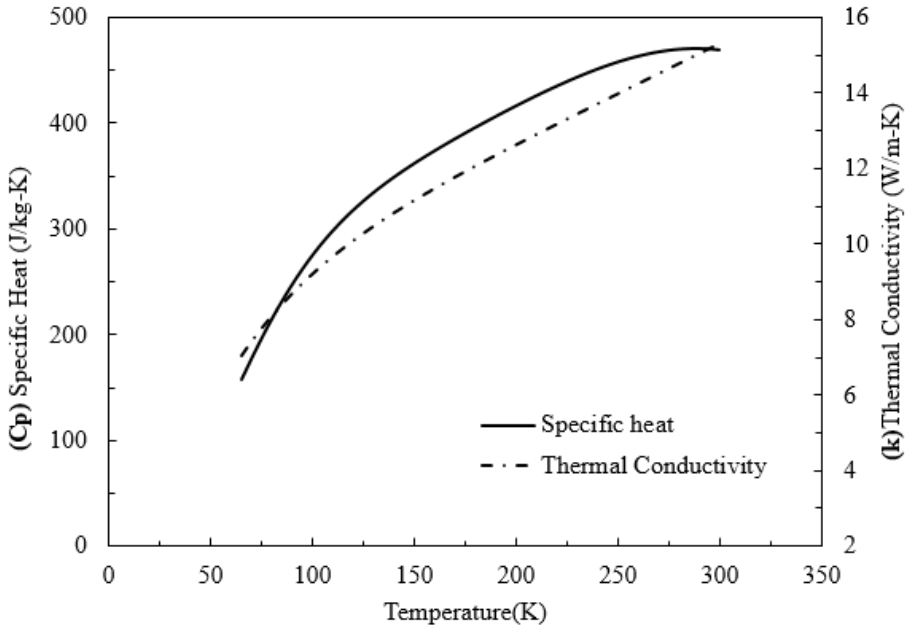

Figure 3.2: Variation of c_p and k with Temperature

	Density (kg/m^3)	**Specific Heat** $(J/g-K)$	**Dynamic Viscosity** $(Pa.s)$	**Thermal Conductivity** $(W/m-K)$
LN_2	806.08	2.0412	1.6×10^{-5}	0.1459
GN_2	Ideal Gas	1.1243	5.43×10^{-6}	0.0075
SS304	8026	P.P.1 3.8	Not-Applicable	P.P.2 3.9

Table 3.2: Thermophysical properties of nitrogen and stainless steel
* P.P - Piece-wise Polynomial

Table 3.2 summarizes the material properties used in the simulations.The properties of Liquid Nitrogen are at saturation and hence these are constant. The previously mentioned polynomial expressions are adapted into the simulations for SS304. Gaseous nitrogen is assumed to be an ideal gas, whose density is calculated by the equation of state. The latent heat of vaporization during phase change is given as 199 kJ/kg.

3.3.3 Initial and boundary conditions

Since it is a transient simulation, the **Initial conditions** are specified as follows :

1. **Fluid Domain :**
   - **Case 1 :** LN_2 at T = 77K
   - **Case 2 :** LN_2 at T = 75K
2. **Solid Domain :**

Boundary Conditions	**Case 1**	**Case 2**
Inlet	Velocity Inlet LN_2 at 77K	Velocity Inlet LN_2 at 75K
Outlet	Gauge Pressure = 0 Pa	Gauge Pressure = 0 Pa
Inner Wall	Coupled Wall	Constant Heat Flux $q = 3000W/m^2$
Outer Wall	Constant Heat Flux $q = 500W/m^2$	Not Applicable

Table 3.3: Boundary Conditions

- **Case 1 :** SS304 at T = 300K

At the inlet, The velocity is varied depending upon the Reynolds number of flow considered. Six different Reynolds numbers are considered. Starting from as low as Re = 500 and proceeding to highest flow rate configuration of Re=50,000, the effect of inlet flow rates on chilldown can be studied. Turbulence model is employed even at low inlet Reynolds number since the local velocity of vapor drastically increases when phase change takes place.In such situations , turbulence cannot be neglected.

The simulations are carried out for all the six Reynolds number at inlet for Case 1. In Case 2 ,only Re = 1500,5000,10000 are considered.

To account for fully developed flow,Entrance length is a necessary parameter. it is a function of Reynolds number and for turbulent regime, it is calculated using the relation given as :

$$L_e = 4.4 \times Re^{\frac{1}{6}} \times d \tag{3.10}$$

However, many authors suggest that the entrance length effects become insignificant when the length is 10 times its diameter.[27] In the current work,the entrance effects are neglected.

3.4 Grid Independence test

A grid independence test is the first and an important step in carrying out a reliable numerical simulations.The methods employed in generating the mesh has to be checked for its accuracy in reproducing similar results for different grid sizes considered.

Three different mesh metrics have been prescribed as an indicator to a good quality mesh. These mesh metrics are as follows:

- Aspect Ratio
- Skewness
- Orthogonal Quality

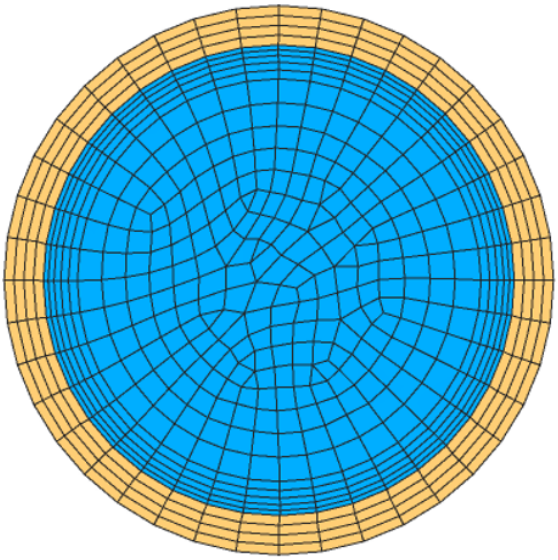

Figure 3.3: Grid used for the Simulations

Aspect Ratio is the ratio between the longitudinal and lateral length of th element. Mesh with elements having Aspect ratio less than 20 is considered to be less error prone. Likewise, Skewness is another important metric and has to be maintained below a value of 0.95.The orthogonal quality of the elements should be as close to 1 as possible. While generating a mesh, not all the elements will have the same value of above mentioned metrics. Hence, it is important to generate more number of elements that do not deviate from the prescribed values of these metrics.

Keeping this in view, various meshing methods have been employed to generate the grid pattern that has been use for the simulations. This is represented in Figure3.3. Inflation layers have been adopted in the fluid domain so that the boundary layer effects are well captured.The solid domain is divided into certain number of radial divisions so that the temperature variation in radial direction can be captured. Inorder to generate different grid sizes, the number of inflation layers and edge sizing have been varied.

The area weighted average properties of velocity and pressure are monitored at two distinct planes for different grid sizes using the same transient time step size employed for the simulations. The simulation is carried out for a considerable number of time steps such that flow phenomena affects the velocity and pressure at considered planes.

The grid independence test is carried out with the same boundary conditions and multiphase flow setup. A high inlet Reynolds number of 100,000 is considered which approximately equates to an inlet flow rate of 0.14 kg/s.

Chapter 4

Results and discussions

4.1 Grid independence outcome

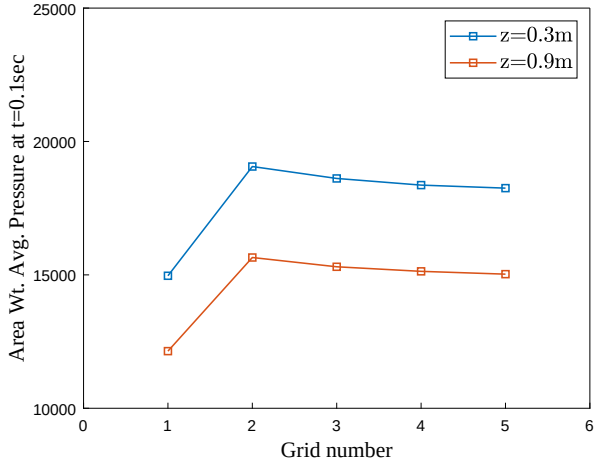

(a) Area Wt Avg. Pressure

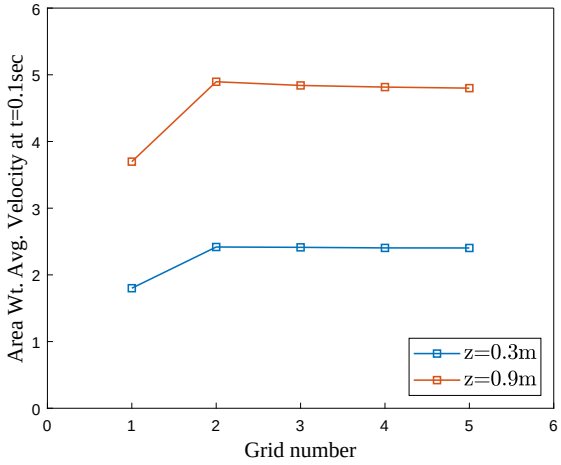

(b) Area Wt Avg. velocity

Figure 4.1: Monitored data at two different planes (t=0.1sec)

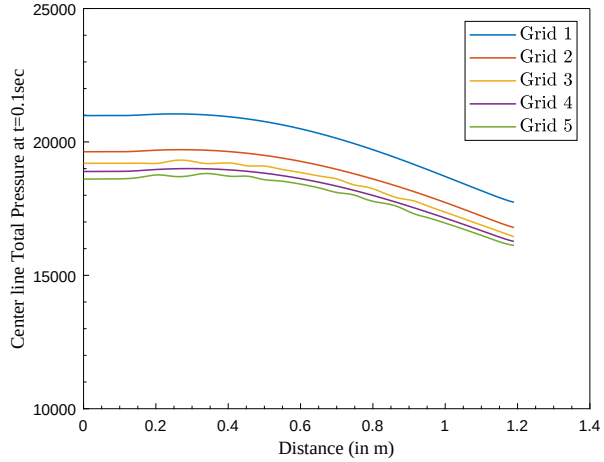

(a) Center line pressure

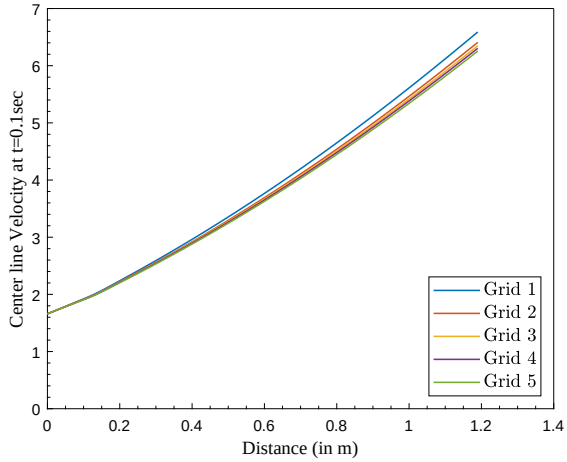

(b) Center line velocity

Figure 4.2: Monitored data across centerline at t=0.1sec

Grid No.	No. of Elements	Area Wt. Avg. Velocity (m/s) (z = 0.3m)	%age error (z = 0.3 m)	Area Wt. Avg. Velocity (m/s) (z = 0.9 m)	%age error (z = 0.9 m)
1	247500	1.800181	-	3.697721	-
2	363500	2.417857	34.3	4.895589	32
3	421848	2.412802	0.2	4.840163	1.1
4	452160	2.404363	0.34	4.815553	0.5
5	520748	2.403292	0.1	4.799781	0.32

Table 4.1: Grid independence data

The center line pressure and velocity variation at t=0.1 sec is shown in Figure 4.2(a),(b) respectively. It is seen that as the grid size increases the deviation in readings assumed a minimum value. For Grid No. 3,4,5 the plot is almost identical. The area weighted average readings of pressure and velocity at two different planes situated at 0.3 m and 0.9m along the longitudinal axis is monitored as well.This is shown in Figure .This also reaffirms the previous observation that variations in data ceases to exist for Grid No's. 3,4,5.Keeping the computational capability in view, Grid No.4 is chosen for the simulation work.

4.2 Overview of analysis domain

Three different planes are considered along the length of the transfer line in order to evaluate various area weighted average properties. These planes are selected such that the effect of flow rate in chilldown phenomena can be easily inferred as flow moves downstream.

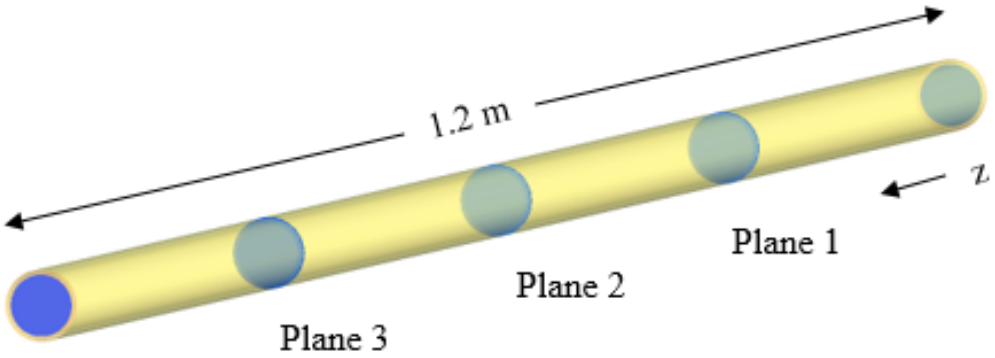

Figure 4.3: Illustration of considered Planes

Figure 4.3 illustrates the positioning of all three planes along the transfer line.Plane 1 represents the upstream section near the inlet where as Plane 3 is the farthest from the inlet ,thereby representing downstream section.All three planes are equidistant from one another such that :

Flow Rate Scenario	Inlet Reynolds number	Mass Flux ($kg/m^2.s$)
Low	500	6.69
Low	1500	20.08
Low	5000	66.9
Moderate	10,000	133.8
High	30,000	401.4
High	50,000	669

Table 4.2: Reynolds number conditions at Transfer line Inlet

- **Plane 1** : z = 0.3 m from inlet
- **Plane 2** : z = 0.6 m from inlet
- **Plane 3** : z = 0.9 m from inlet

4.3 Property Distribution Contours of Case 1

Case 1 refers to the situation when the transfer line is initially at 300K with liquid nitrogen at 77K passing through it.The heat capacity of the wall acts as a heat source to the flowing cryogen. The contours of Vapor, Velocity, Pressure and Temperature distribution across all three planes are included at different times.This will provide an insight in variation of these properties as time progresses. Also, the effect of flow rate on chilldown phenomena can be studied through these contours. High pressure surges can be seen at high Reynolds number at inlet.Circumferential Temperature distribution of the wall cases to exist as flow rate decreases. Presence of vapor in the line can be analyzed from vapor distribution contours.

Inorder to accurately gauge the effect of inlet flow rate, different inlet velocities of liquid nitrogen are considered.The corresponding Reynolds number at inlet is used for better depiction.Table 4.2 refers to the different flow rate scenarios categorized depending upon the inlet Reynolds number.

Initially when the cryogen is at 77K, rapid heat flux enters from the walls resulting in boiling. Vapor generated subsequently attains higher velocities because of its high expansion ratio.Owing to its lower density, vapor reaches the top portions of the line.This phenomena can be seen at all flow rates.However, the amount of vapor generated is greatly influenced by flow rate and is explained in further sections.In the following sections, the contours of velocity,pressure, volume fraction and temperature are provided for each of the different inlet Reynolds number considered.This would serve as a representative of how the above mentioned properties vary across the transfer line.

4.3.1 Contours of inlet G $= 6.69$ kg/m^2.s

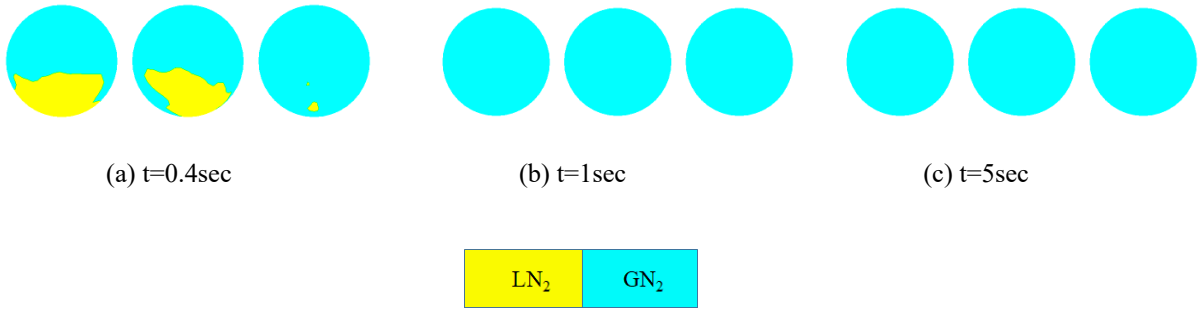

(a) t=0.4sec (b) t=1sec (c) t=5sec

(d) Volume fraction

Figure 4.4: Vapor distribution across planes ($G = 6.69\ kg/m^2.s$)
Plane 1(left) - Plane 3(right)

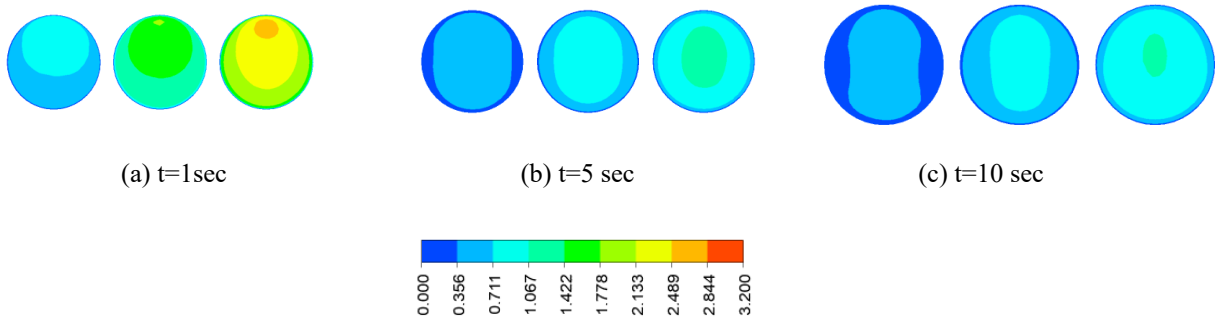

(a) t=1sec (b) t=5 sec (c) t=10 sec

(d) Velocity(m/s)

Figure 4.5: Velocity distribution across planes ($G = 6.69\ kg/m^2.s$)
Plane 1 (left)- Plane 3 (right)

The inlet mass flux of 6.69 $kg/m^2.s$ usually indicates laminar regime.However,at the downstream sections gaseous nitrogen velocity can reach very high values because of its high volumetric expansion.These observations are made from Figure 4.5. As a result,turbulence effects come into picture and for that reason the turbulence equations of $k-\epsilon$ are considered for laminar Reynolds number as well. From Figure 4.4, it is important ot note the presence of vapor for most duration of the chilldown phenomena. Since the mass flux is very low at inlet,incoming liquid nitrogen boils off imminently even before reaching the upstream plane-1. The vapor generated as a result of phase change moves downstream slowly and at any given instant of t> 1sec,all three planes show presence of single phase gaseous nitrogen. Gaseous nitrogen proceeds downstream for longer periods until wall reaches cryogenic temperatures.

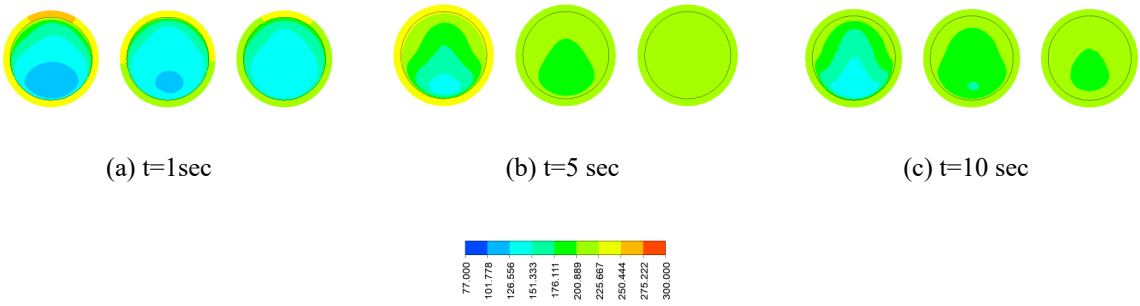

(a) t=1sec (b) t=5 sec (c) t=10 sec

(d) Volume fraction

Figure 4.6: Temperature distribution across planes ($G = 6.69\ kg/m^2.s$)
Plane 1 (left)- Plane 3 (right)

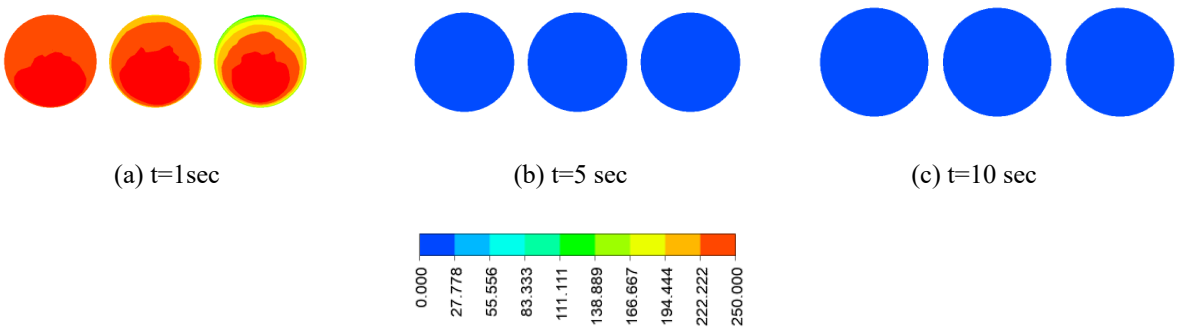

(a) t=1sec (b) t=5 sec (c) t=10 sec

(d) Pressure (Pa)

Figure 4.7: Pressure distribution across planes ($G = 6.69\ kg/m^2.s$)
Plane 1 (left)- Plane 3 (right)

Figure 4.6 shows a uniform temperature distribution on the wall which is not the case at high flow rates.This reiterates the fact that the presence of a single phase gaseous nitrogen cools down the wall uniformly.At higher flow rates presence of stratified flow shows deviation form this behavior.

4.3.2 Contours of inlet G = 20.08 kg/m^2.s

At low inlet mass flux of 6.69, 20.08 and 66.9 $kg/m^2.s$ there is very minimal pressure surge.As time progresses, pressure inside the line evens out as the heat transfer rates decreases with wall temperature drop. This can be seen from contours of Figure 4.7, 4.10, 4.14. Liquid nitrogen initially in the line is vaporized and is replaced by incoming fluid.Since the velocity of incoming liquid Nitrogen is too low, there is ample amount of contact time with the wall.This results in instant vaporization of incoming liquid nitrogen at the upstream sections itself.Such scenario leads to the presence of single phase gaseous nitrogen for most part of the line.Single phase gaseous convection takes place whereas at higher flow rates two

(a) t=0.4sec (b) t=1sec (c) t=5 sec

(d) Volume fraction

Figure 4.8: Vapor distribution across planes ($G = 20.08\ kg/m^2.s$)
Plane 1 (left)- Plane 3 (right)

phase flow boiling existed.This phenomena is specific to low inlet Reynolds number and can be visualized from Figures 4.8, 4.4 , 4.12.

(a) t=1sec (b) t=5 sec (c) t=10 sec

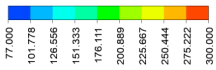

(d) Volume fraction

Figure 4.9: Temperature distribution across planes ($G = 20.08\ kg/m^2.s$)
Plane 1 (left)- Plane 3 (right)

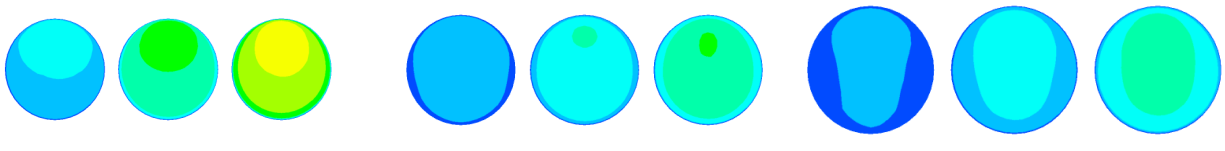

(a) t=1sec (b) t=5 sec (c) t=10 sec

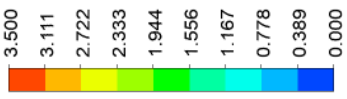

(d) Velocity(m/s)

Figure 4.11: Velocity distribution across planes ($G = 20.08\ kg/m^2.s$)
Plane 1 (left)- Plane 3 (right)

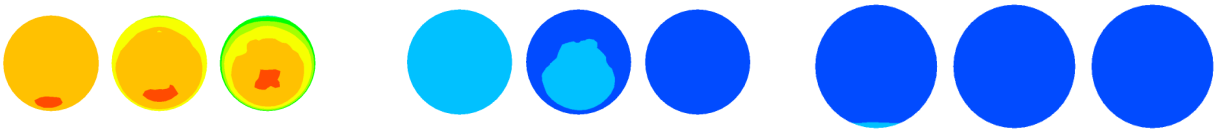

(a) t=1sec (b) t=5 sec (c) t=10 sec

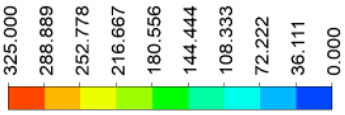

(d) Pressure (Pa)

Figure 4.10: Pressure distribution across planes ($G = 20.08\ kg/m^2.s$)
Plane 1 (left)- Plane 3 (right)

Figure 4.10 and 4.11 show the distribution of pressure and velocity magnitude at mass flux of $20.08\ kg/m^2.s$ respectively. At t = 10 sec, the pressure distribution in the line is very uniform since single phase gaseous nitrogen existed throughout the line. Absence of phase change at these sections shows no pressure surges in the line.

4.3.3 Contours of inlet G $= 66.9$ kg/m^2.s

(a) t=0.4sec (b) t=1 sec (c) t=5sec

(d) Volume fraction

Figure 4.12: Vapor distribution across planes ($G = 66.9\ kg/m^2.s$)
Plane 1 (left)- Plane 3 (right)

Contours of velocity from Figures 4.5, 4.11, 4.15 bear a common significance. The top portions of the line reach higher velocities at t=1sec since the initially present liquid nitrogen vaporizes. However this scenario cease to exist with time. Since gaseous nitrogen engulfs the transfer line completely , a single phase flow situation arises and the velocity contour approximately resembles the turbulent velocity profile.

(a) t=1sec (b) t=5 sec (c) t=10 sec

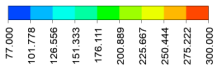

(d) Volume fraction

Figure 4.13: Temperature distribution across planes ($G = 66.9\ kg/m^2.s$)
Plane 1 (left)- Plane 3 (right)

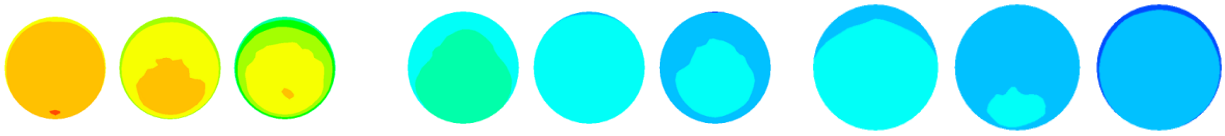

(a) t=1sec (b) t=5 sec (c) t=10 sec

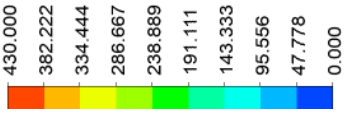

(d) Pressure (Pa)

Figure 4.14: Pressure distribution across planes ($G = 66.9\ kg/m^2.s$)
Plane 1 (left)- Plane 3 (right)

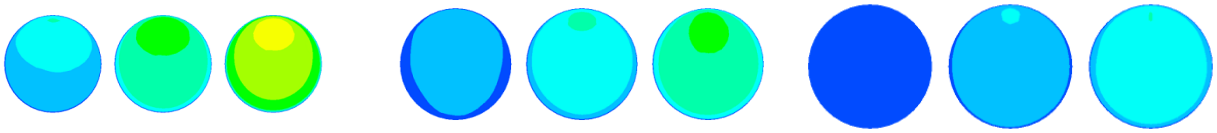

(a) t=1sec (b) t=5 sec (c) t=10 sec

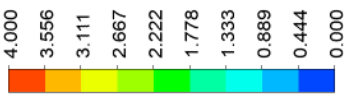

(d) Velocity(m/s)

Figure 4.15: Velocity distribution across planes ($G = 66.9\ kg/m^2.s$)
Plane 1 (left)- Plane 3 (right)

4.3.4 Contours of inlet G = 133.8 kg/m^2.s

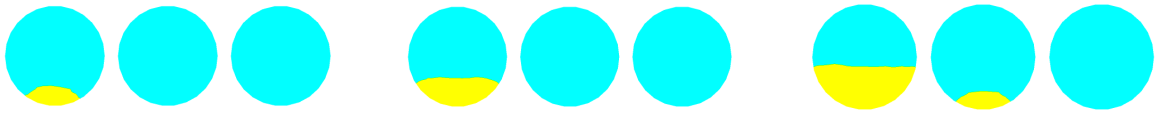

(a) t=1sec (b) t=5 sec (c) t=10 sec

(d) Volume fraction

Figure 4.16: Vapor distribution across planes ($G = 133.8\ kg/m^2.s$)
Plane 1 (left)- Plane 3 (right)

These contours represent a moderate flow rate scenario. Figure 4.16 shows the distribution of vapor and liquid in the transfer line at different times. It can be seen that the line is initially filled with liquid Nitrogen instantly vaporizes thereby forming a large amount of vapor. At t=10sec liquid nitrogen starts to appear at plane 2. This shows that as the flow rate increases, liquid nitrogen flows more rapidly towards downstream and would have lesser contact time with the wall. At plane 1, it can be seen that the amount of liquid nitrogen increases with time.This is facilitated because of temperature drop at those sections leading to lower heat transfer rates. Unlike low flow rate scenarios, a circumferential distribution of wall temperature can be seen from Figure 4.17.This confirms the presence of two phase flow propagating downstream with time. Liquid nitrogen flows at the bottom portions because of its higher density. As a result,lower portions chilldown faster.

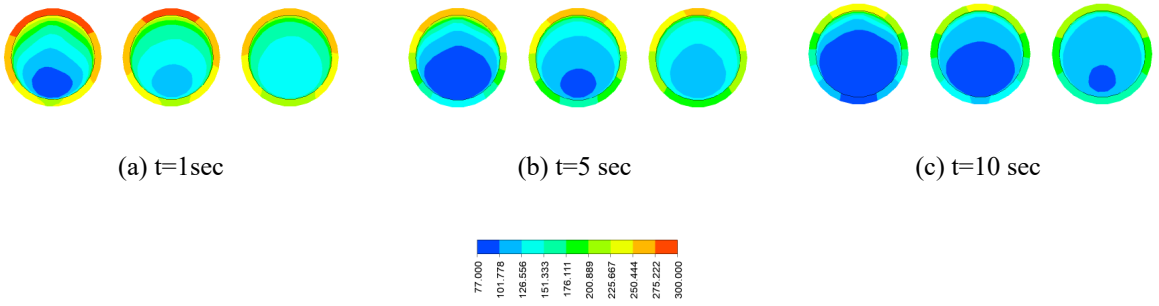

(a) t=1sec (b) t=5 sec (c) t=10 sec

(d) Volume fraction

Figure 4.17: Temperature distribution across planes ($G = 133.8\ kg/m^2.s$)
Plane 1 (left)- Plane 3 (right)

On the other hand, low thermal conductivity vapor occupies the top portions of the line which impedes the heat transfer rate. It can be seen that the LN2 temperatures reach a

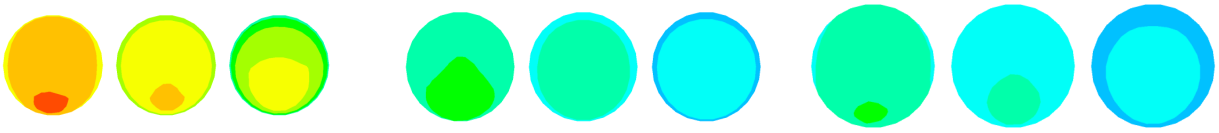

(a) t=1sec (b) t=5 sec (c) t=10 sec

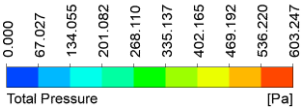

(d) Pressure (Pa)

Figure 4.18: Pressure distribution across planes ($G = 133.8\ kg/m^2.s$)
Plane 1 (left)- Plane 3 (right)

maximum of 77K after which it changes to gaseous phase. This gaseous nitrogen, at times, exists in super-heated state and reaches temperatures of 150K.

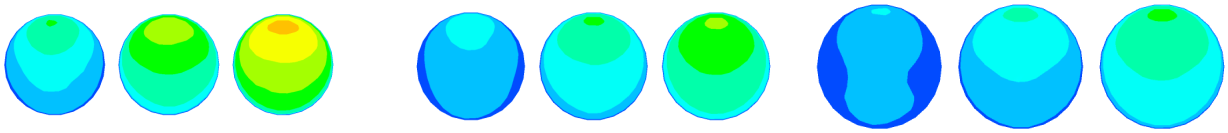

(a) t=1sec (b) t=5 sec (c) t=10 sec

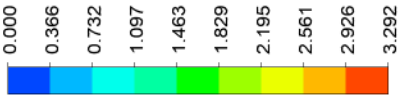

(d) Velocity(m/s)

Figure 4.19: Velocity distribution across planes ($G = 133.8\ kg/m^2.s$)
Plane 1 (left)- Plane 3 (right)

. Figure 4.19 illustrates the flow velocity inside the transfer line at different times. It can be seen at the downstream planes, local velocities reach a higher value , specifically at the top portions.This increase in velocity is accompanied by drop in pressure. The vapor reaches top sections and as it travels downstream most of the pressure energy gets converted to kinetic energy.

4.3.5 Contours of inlet G $= 401.4$ kg/m^2.s

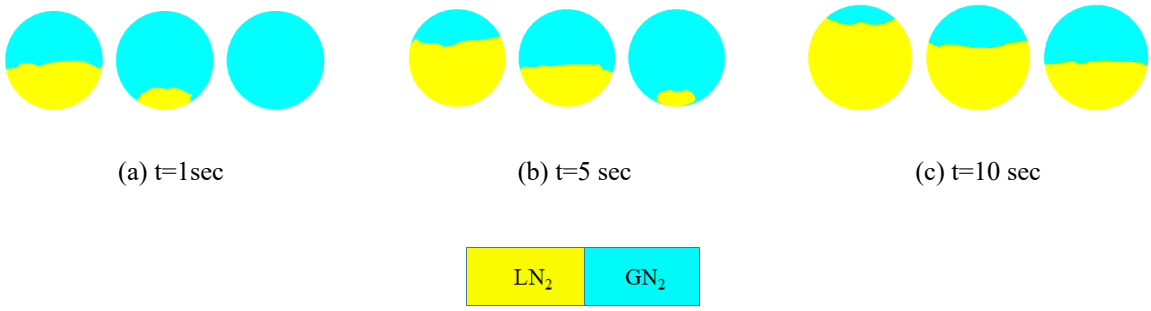

(a) t=1sec (b) t=5 sec (c) t=10 sec

(d) Volume fraction

Figure 4.20: Vapor distribution across planes ($G = 401.4\ kg/m^2.s$)
Plane 1 (left)- Plane 3 (right)

Figure 4.20 and 4.24 show the distribution of gaseous nitrogen at an inlet mass flux of 401.4 and 669 $kg/m^2.s$ respectively. At such high flow rates, liquid nitrogen rushes into the transfer line displacing the generated vapor.at t=10 sec it can be seen that the liquid nitrogen has already accumulated at the bottom portions of the line. Liquid nitrogen doesn't have sufficient time to be in contact with the wall thereby resulting in low vapor presence at any particular instant of time. Figure 4.22 and 4.23 show the pressure and velocity magnitudes along the transfer line. As mentioned earlier,gaseous nitrogen attains higher velocities and its magnitude increases along the transfer line.

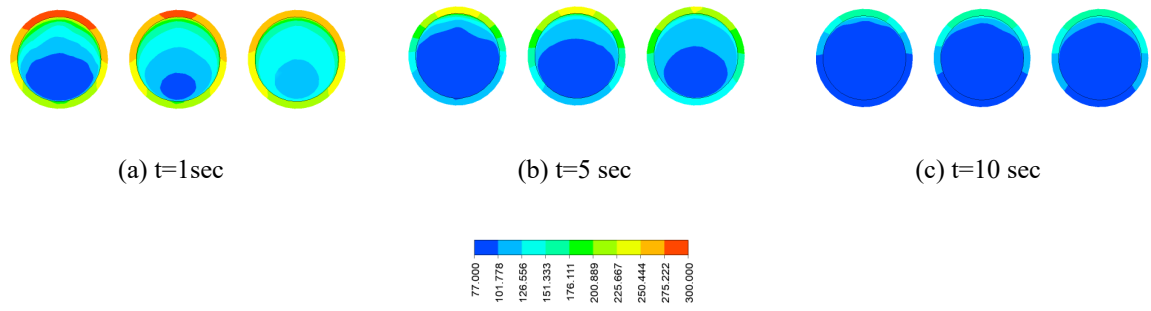

(a) t=1sec (b) t=5 sec (c) t=10 sec

(d) Volume fraction

Figure 4.21: Temperature distribution across planes ($G = 401.4\ kg/m^2.s$)
Plane 1 (left)- Plane 3 (right)

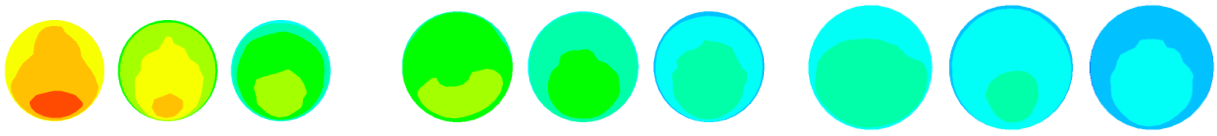

(a) t=1sec (b) t=5 sec (c) t=10 sec

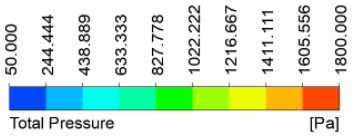

(d) Pressure (Pa)

Figure 4.22: Pressure distribution across planes ($G = 401.4\ kg/m^2.s$)
Plane 1 (left)- Plane 3 (right)

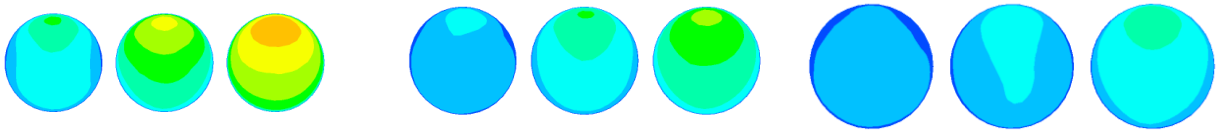

(a) t=1sec (b) t=5 sec (c) t=10 sec

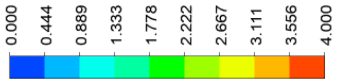

(d) Velocity(m/s)

Figure 4.23: Velocity distribution across planes ($G = 401.4\ kg/m^2.s$)
Plane 1 (left)- Plane 3 (right)

4.3.6 Contours of inlet G $= 669\ \mathbf{kg/m^2.s}$

Figure 4.26shows the gauge pressure distribution along the transfer line at different times. At t=1sec, when the bulk fluid evaporates as a result of rapid heat flux, there is a high pressure surge in the system. As liquid nitrogen starts flowing the pressure surge eventually decreases as heat flux into the system reduces. These pressure surges are very high in case of high flow rates and have a considerable effect on local saturation temperature of fluid. In order to account for this phenomena, the variation of saturation temperature with pressure is considered as a piece wise polynomial function.

Figure 4.21 and 4.25 show the temperature distribution at high inlet mass flux of 401.4 and 669 $kg/m^2.s$ respectively.The temperature variation in the circumferential plane is more evident at these flow rates. The difference in temperature at top and bottom portions reach as high as 100K. This would have adverse effects on heat transfer coefficients encountered at those respective portions. Initially present liquid nitrogen vaporizes quickly and is displaced by flowing liquid nitrogen.hence two phase flow exists for majority of the duration. At

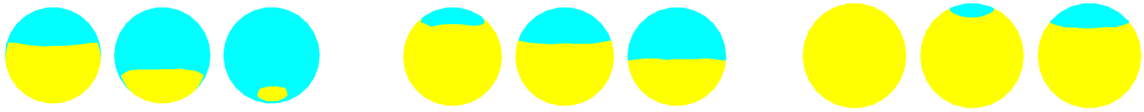

(a) t=1sec (b) t=5 sec (c) t=10 sec

(d) Volume fraction

Figure 4.24: Vapor distribution across planes ($G = 669\ kg/m^2.s$)
Plane 1 (left)- Plane 3 (right)

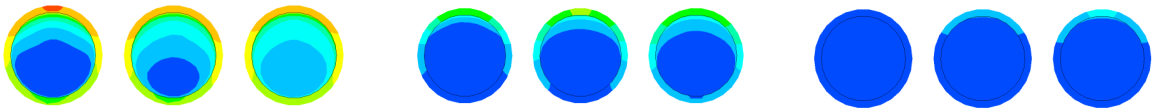

(a) t=1sec (b) t=5 sec (c) t=10 sec

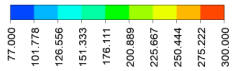

(d) Volume fraction

Figure 4.25: Temperature distribution across planes ($G = 669\ kg/m^2.s$)
Plane 1 (left)- Plane 3 (right)

t=10 sec, it can be seen that the downstream sections (plane 3) are nearly at 77K. This also reiterates the fact that liquid nitrogen flows faster with minimal vapor presence at any instant of time. At any instant of time , the circumferential variation of temperature can be observed at higher flow rates as well. However, the top portions of upstream sections (Plane 1) still remain at higher temperatures than the downstream sections. This is counter intuitive since it is expected that the upstream sections chilldown faster. This effect slowly diminishes as liquid nitrogen flows through the line.

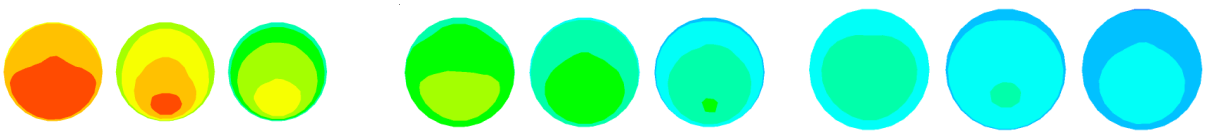

(a) t=1sec (b) t=5 sec (c) t=10 sec

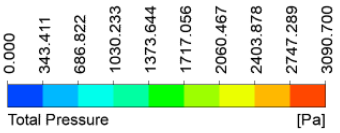

(d) Pressure (Pa)

Figure 4.26: Pressure distribution across planes ($G = 669\ kg/m^2.s$)
Plane 1 (left)- Plane 3 (right)

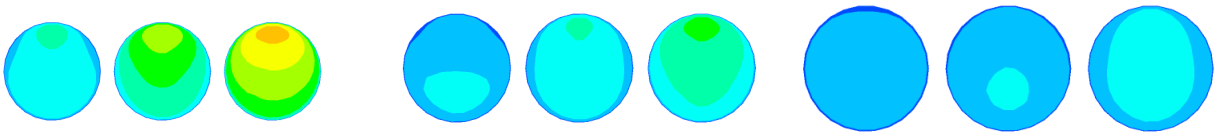

(a) t=1sec (b) t=5 sec (c) t=10 sec

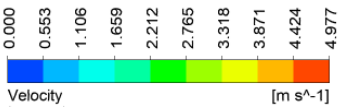

(d) Velocity(m/s)

Figure 4.27: Velocity distribution across planes ($G = 669\ kg/m^2.s$)
Plane 1 (left)- Plane 3 (right)

(a) ($G = 6.69\ kg/m^2.s$)

(b) ($G = 20.08\ kg/m^2.s$)

(c) ($G = 66.9\ kg/m^2.s$)

Figure 4.28: Vapor distribution at mid section at t = 5 sec (low mass flux)

A sectional view of the transfer line along its length as in Figures 4.29 and 4.28 show the liquid-vapor distribution at t=5sec. With increasing flow rate , the amount of liquid nitrogen

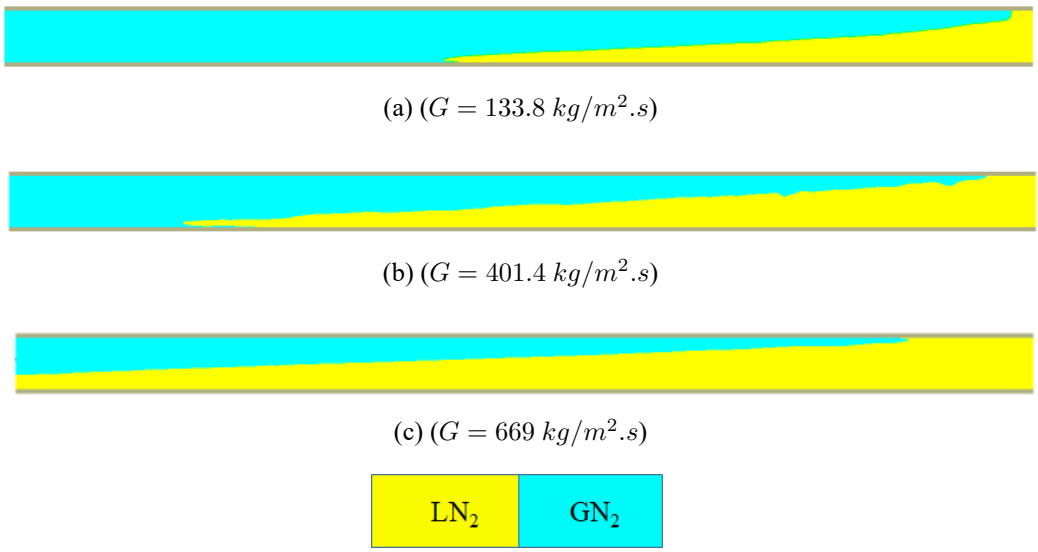

Figure 4.29: Vapor distribution at the mid section at t = 5 sec (high mass flux)

in the line increases. Also, at low inlet Reynolds number, the transfer line is totally filled with gaseous nitrogen.Two phase flow assumes stratified flow pattern at higher flow rates with vapor reaching the top portions as a result of buoyancy

4.4 Area weighted Average Properties

Case 1: Area weighted average properties of temperature,velocity and pressure at different planes helps in understanding the flow phenomena occurring along the line. Presence of single phase gas convection at downstream sections can be identified by measuring the weighted average values of temperature and volume fraction. Pressure and velocity vary along the transfer line and especially the increase in velocity is accompanied a drop in pressure at any given cross section.This phenomena can be observed by measuring the area weighted average values of pressure and velocity.

Once the leidenfrost point is reached, the boiling regimes hifts from boiling to Nucleate. Film boiling, which was studied in this case, is charecterized by high wall superheat (Tw-Tf). Initially, when the liquid cryogen completely occupies the transfer line, high wall heat fluxes are encountered. With time, these wall heat fluxes decrease. When regime shifts to nucleate, nucleation sites starts appearing in the flow.At this point, liquid cryogen starts coming into contact with the wall therby resulting in high heat transfer rate. The wall temperature takes an abrupt hit to near cryogenic temperatures. When this regime ends, single phase gas convection exists. Since majority of the chilldown phenomena exists in film boiling, Leidenfrost point becomes an important parameter in identifying the change in regime.The temperature at which this change happens is termed as Leidenfrost point / Minimum Film Boiling temperature / Rewetting temperature.

Carbajo [28] studied rewetting temperatures to estimate re-flooding in a LWR(light water reactor) He proposed the Leidenfrost temperature to be a function of Critical temperature and saturation temperature of cryogen. 4.1.

$$T_{Leid} = \frac{T_{cr} - T_{\text{sat}}}{K\sqrt{\mu_f}}(1+\beta) + T_{\text{sat}} \tag{4.1}$$

However, some authors have proposed that the hydrodynamic effects of flow have a considerable role in transition of regime. Alternatively, The Leidenfrost temperature was expressed as a function of mass flux at the inlet and is expressed by De Salve, M. and Panella,B [29].

Unless the flow rates are very high which would mean high inlet pressures, the effect of these hydrodynamic properties are negligible at the mass flux considered in this work. Th Leidenfrost temperature is estimated to be within 5K of 130K even if the hydrodynamic effects are considered.

4.4.1 Variation of weighted average properties

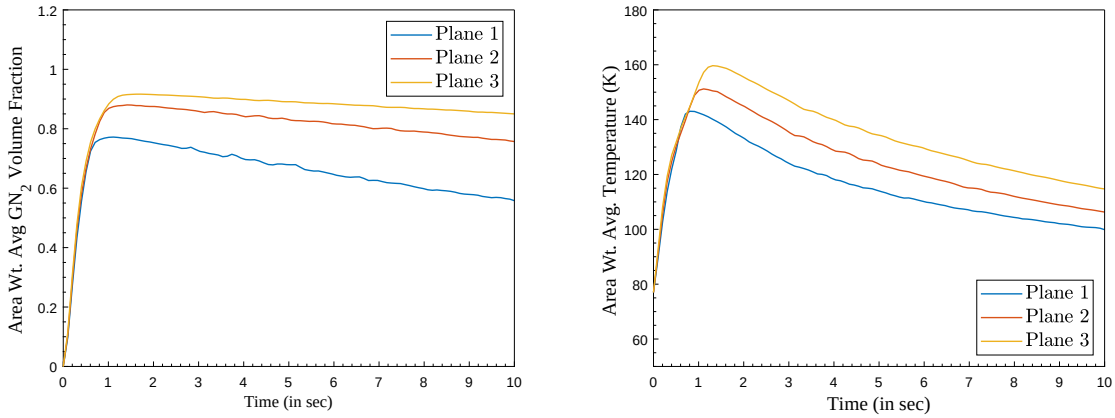

(a) Volume fraction of GN_2

(b) Temperature

Figure 4.30: Variation of weighted average properties at $G = 133.8\ kg/m^2.s$

The variation of gaseous nitrogen with time and temperature of the fluid domain at three different planes are shown in Figures 4.30a and 4.30b.As the distance from inlet increases more vapor gets accumulated since the flowing cryogen carries bulk of the heat and changes its phase. As a consequence, the temperature at downstream planes are higher. In this work plane 3 is representative of downstream section.Similar explanation can be given for flows involving high mass flux at inlet as well.The behavior of flow phenomena at low mass flux is explained further with the help of comparative study of weighted properties.

4.4.2 Comparative studies on weighted average properties

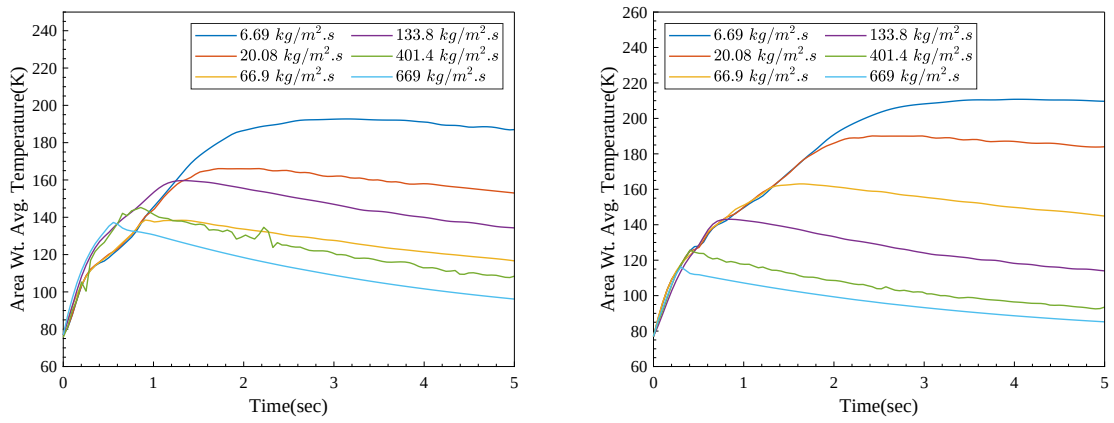

(a) (b)

Figure 4.31: Temperature variation of fluid at different mass flux

Figure 4.31a;4.31b show the variation of weighted average temperature distribution at plane 1 and plane 2 respectively.The initial surge in temperatures is due to the fact that liquid cryogen is already present in the line.At low flow rates, since the liquid cryogen has longer time to interact with the all, it reaches a higher peak value.It can also be seen that the average temperature at a plane reduces with increasing flow rate. Incoming liquid cryogen that is at 77K with a higher flow rate tend to reduce the average temperature.This phenomena would effectively result in low presence of gaseous nitrogen at any particular plane and a time instant.This variation can be seen from Figure 4.32a,4.32b.

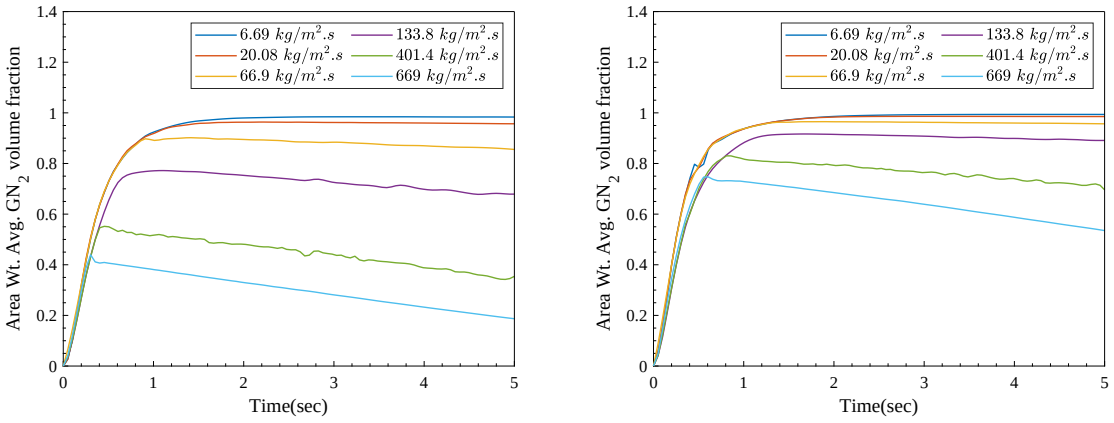

(a) (b)

Figure 4.32: Weighted Average GN_2 volume fraction at different mass flux

At plane 1 , relatively low vapor is present at any flow rate. as phase change takes place, more vapor is accumulated at plane 2 since, the heat transfer area to reach the plane

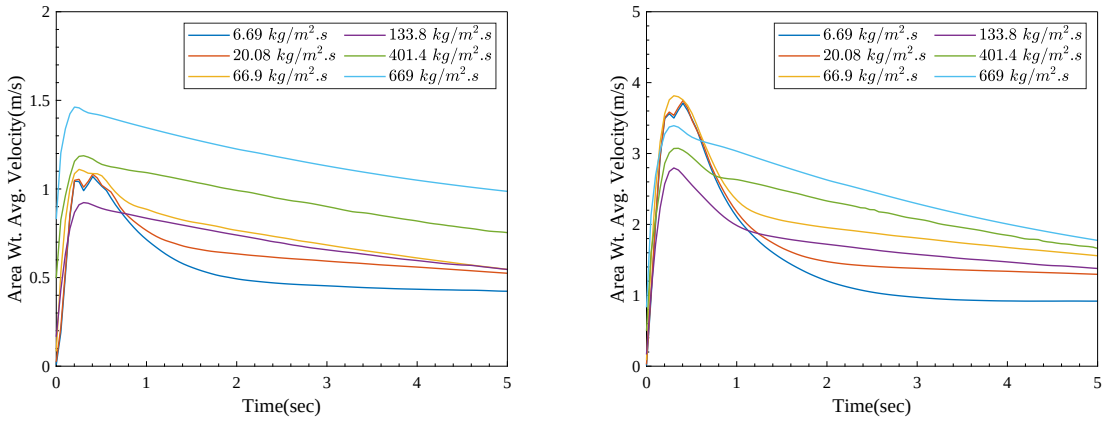

Figure 4.33: Weighted Average velocity at different mass flux

is higher.With higher flow rates, the velocity of resulting gaseous nitrogen is high enough to quickly escape the transfer line.This variation can be seen in Figure 4.33a,4.33b.The gaseous phase attains higher velocities owing to its high expansion ratio during phase change.Also , the velocity of incoming fluid is so high and it replaces the gaseous phase at a faster rate. This phenomena become more pronounced as flow rate increases.Hence, a snapshot of an arbitrary plane has lesser amounts of gaseous phase at higher flow rates.

4.5 Chilldown Characteristics

Important consideration of any chilldown process is to estimate the time taken to cooldown the transfer line. In most of the cases, time taken for the downstream sections of the line to cooldown is considered to be the representative of chilldown time. A time history plot of temperature measured at a certain location in the line called chilldown curve, provides insight into the shift of boiling regimes occurring during this phenomena.

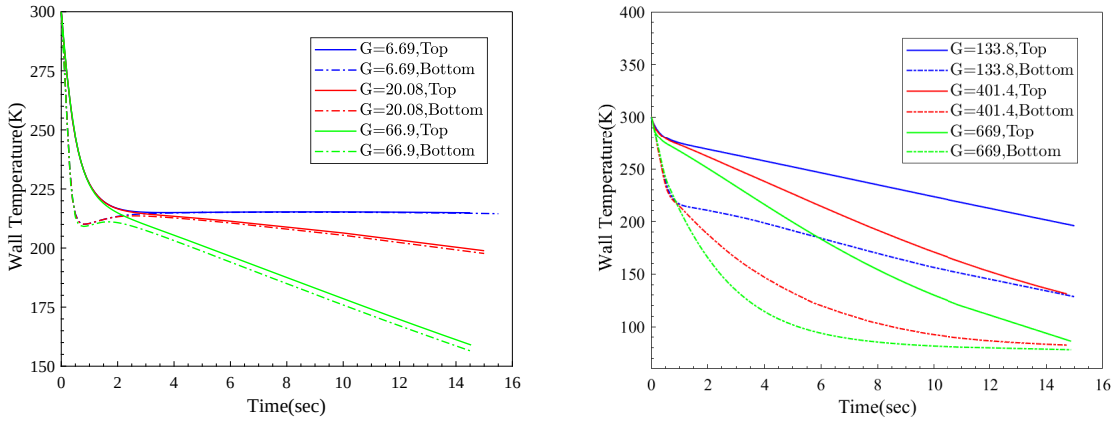

(a) (b)

Figure 4.34: Temperature history at the outer wall of downstream section

Figure 4.34 shows the variation of temperature at the outermost radius of transfer line at downstream section(z = 0.9m). Figure 4.34a shows the variation at low mass flux whereas 4.34b depicts high mass flux. The top and bottom portions denote $\theta = 90°, 180°$.These points are considered so that the presence of circumferential temperature variance can be confirmed.At lower mass flux , it is observe that the top and bottom portions are almost at the same temperature. In fact, circumferential variation is absent at low flow rates due to the presence of single phase gaseous nitrogen for most of the time.Owing to its, low thermal conductivity, it takes much longer for transfer line to cooldown. However, at higher mass flux , there is a considerable temperature difference between top and bottom portions.The bottom portions cooldown faster as compared to top portions.Presence of two phase flow at downstream sections is the reason for this circumferential temperature distribution.

Figure 4.35 depicts the outer wall temperature of the transfer line at t = 10 sec. The wall cools down faster when the flow rate is high as in the case of 4.35(f). Uniform temperature distribution across a cross section can be seen for low flow rates such as 4.35(a),(b),(c).

In chilldown process, the properties of fluid do not remain constant.As gaseous phase presence increases downstream, thermal conductivity changes.As a result, conduction resistance increases.Heat transfer from the inner wall is of very high magnitude that the residual heat leaks into the system can be neglected.

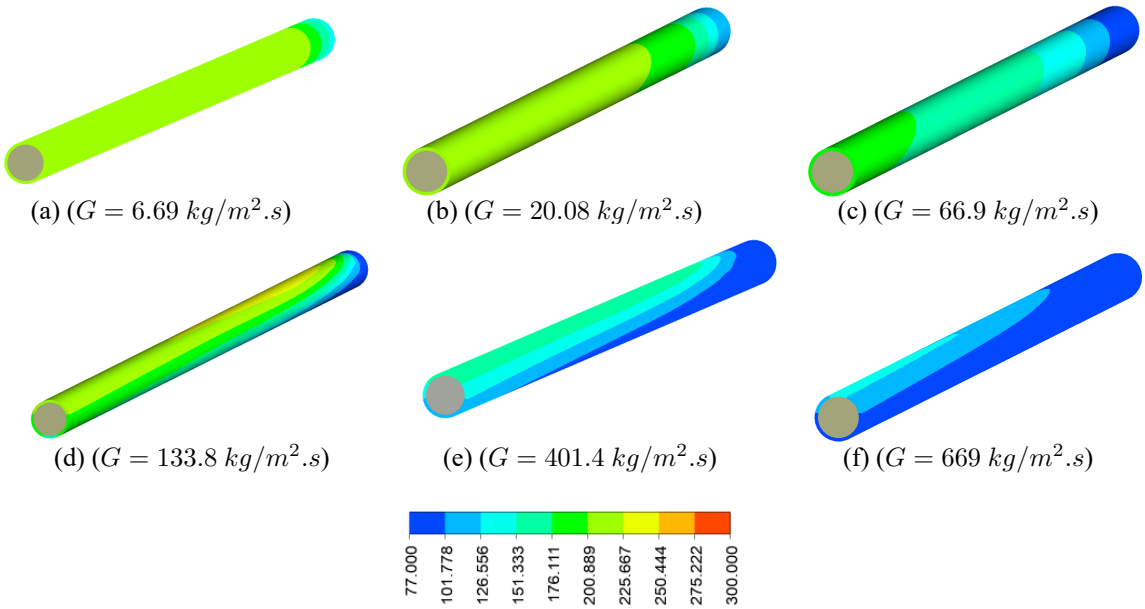

(a) ($G = 6.69\ kg/m^2.s$) (b) ($G = 20.08\ kg/m^2.s$) (c) ($G = 66.9\ kg/m^2.s$)

(d) ($G = 133.8\ kg/m^2.s$) (e) ($G = 401.4\ kg/m^2.s$) (f) ($G = 669\ kg/m^2.s$)

(g) Temperature(K)

Figure 4.35: Temperature distribution on the Outer wall (t=10sec)

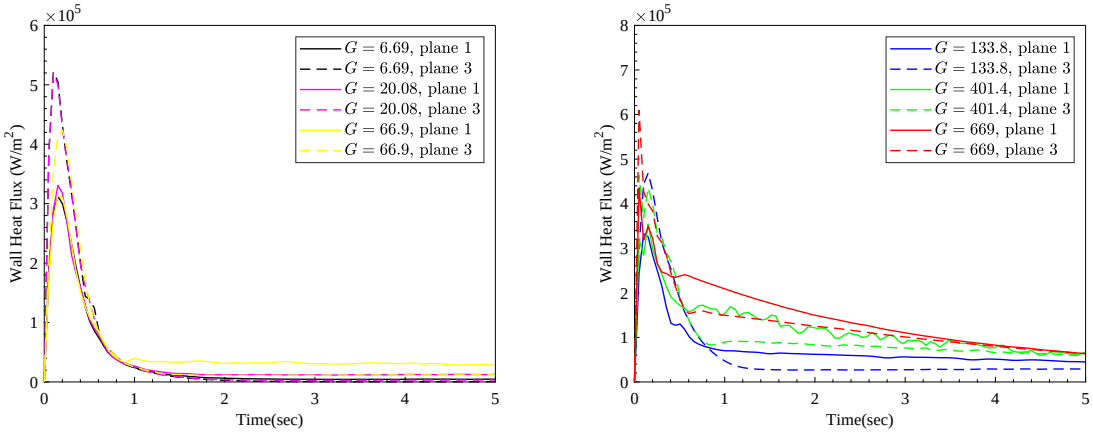

(a) $q\ vs\ t$ at low mass flux (b) $q\ vs\ t$ at high mass flux

Figure 4.36: Wall heat flux history for different planes

Since the transfer line is assumed to be filled with liquid nitrogen initially, the extreme temperature difference results in high heat flux.These peak readings increase with increasing mass flux. However, as gaseous phase starts forming and occupy entirety of the line,especially at low mass flux, the heat flux decreases owing low thermally conductive gas.These values are similar at upstream and downstream locations.As shown in Figure4.36b, the same inference isn't valid at high mass flux. Rapid flow of liquid cryogen with relatively larger thermal conductivity diffuse the heat more quicker thereby leading to high heat flux.Even at downstream sections these values are large as the average temperature of flow is lower.It causes faster chilldown and as the wall superheat reduce, the heat flux into

the system eventually dies down.The heat transfer coefficients during the initial surge reach to values of $10\ kW/m^2 - K$. Thermal conductivity of existing fluid drops along the transfer line when gaseous phase is existent. As wall temperature drops and liquid nitrogen proceeds towards downstream locations , it results in nucleate boiling where wall eventually reaches cryogenic temperatures.

4.6 Results of Flow phenomena (problem case 2)

In this problem,the thickness of transfer line isn't considered. When chilldown takes place and the line assumes steady state operation, there still might be heat leaks from the surroundings.Transfer line might have already reached near cryogenic temperatures but presence of heat leaks can lead to phase change of liquid cryogen. The contours of liquid-vapor distribution, temperature at different flow rates are included further.

4.6.1 Vapor distribution

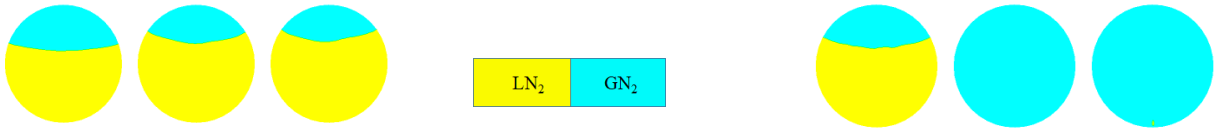

(a) t = 3 sec (c) t = 5 sec

Figure 4.37: Vapor distribution contours ($G = 20.08\ kg/m^2.s$)
Plane 1 (left) - Plane 3 (right)

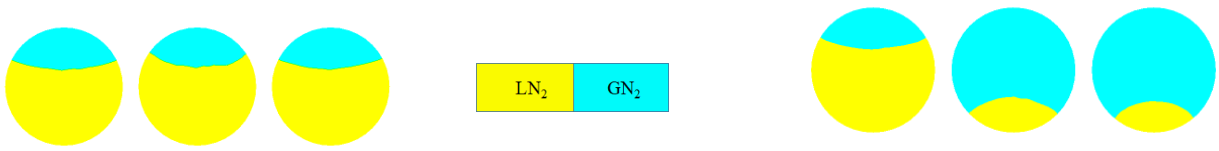

(a) t = 3 sec (c) t = 5 sec

Figure 4.38: Vapor distribution contours ($G = 66.9\ kg/m^2.s$)
Plane 1 (left) - Plane 3 (right)

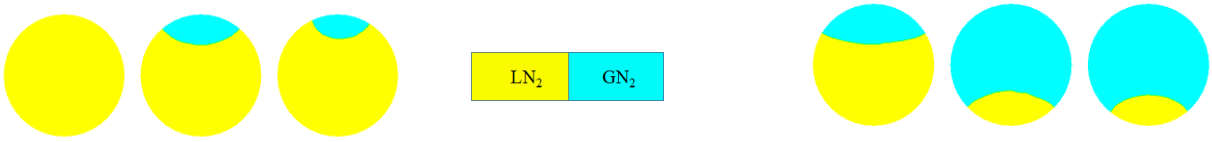

(a) t = 3 sec

(c) t = 5 sec

Figure 4.39: Vapor distribution contours ($G = 133.8\ kg/m^2.s$)
Plane 1 (left) - Plane 3 (right)

From Figures 4.37 , 4.38 4.39, the presence of vapor as we move downstream from plane 1 to plane 3 can be seen for all mass fluxes as time progresses.

4.6.2 Temperature distribution

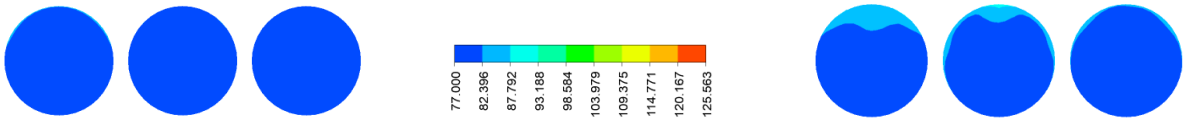

(a) t = 3 sec

(c) t = 5 sec

Figure 4.40: Temperature contours($G = 20.08\ kg/m^2.s$)
Plane1 (left) - Plane3 (right)

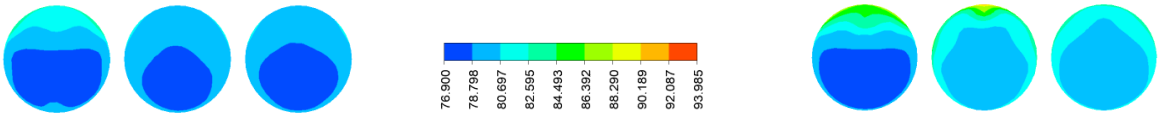

(a) t = 3 sec

(c) t = 5 sec

Figure 4.41: Temperature contours $G = 66.9\ kg/m^2.s$
Plane1 (left) - Plane3 (right)

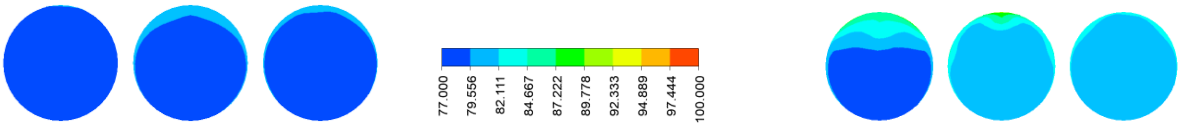

(a) t = 3 sec

(c) t = 5 sec

Figure 4.42: Temperature contours $G = 133.8\ kg/m^2.s$
Plane1 (left) - Plane3 (right)

Figure 4.40, 4.41,4.42, represent the temperature distribution at all three planes for different inlet mass flux. As vapor reaches the top section,the gaseous temperature is more than 77K.The temperatures within vicinity of liquid cryogen do not exceed 77K.

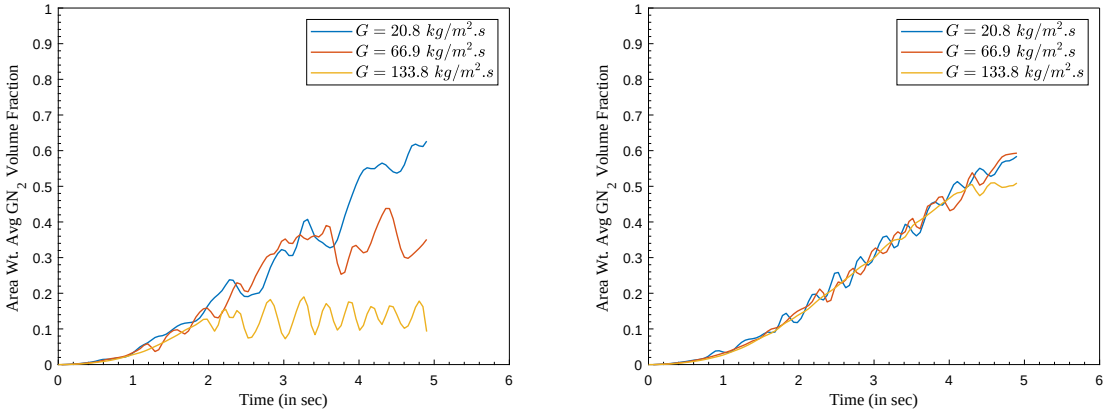

(a) Plane 1 (b) Plane 3

Figure 4.43: Area wt. Avg. GN2 volume fraction at different mass flux.

Figure 4.43a , 4.43b show the variation of gaseous phase volume fraction for different mass flux at plane 1 and plane 3 respectively.The presence of gaseous nitrogen at upstream plane decreases as mass flux increases.It is intuitive that incoming liquid cryogen with a higher velocity would decrease the overall presence of gaseous nitrogen. However, at downstream sections the gaseous phase is found to be independent of mass flux.The fluctuated form of variation is owing to the presence of vapor bubble adhering to the top portions and propagating downstream. These would eventually collapse as flow moves downstream owing to heat transfer.

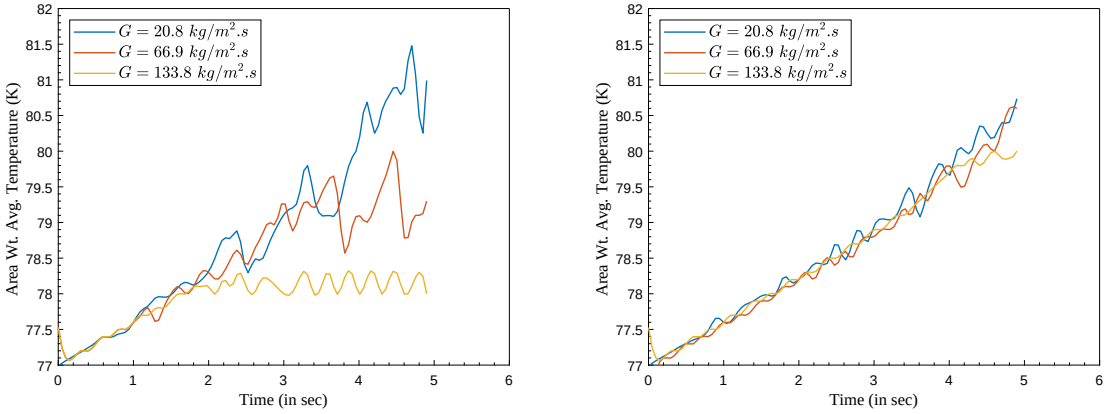

(a) Plane 1 (b) Plane 3

Figure 4.44: Area wt. Avg. Temperature at different mass flux.

The distribution in figure 4.44a , 4.44b show that higher temperatures oscillations are

more prevalent at plane 1. However, for low mass flux, gaseous cryogen reaches higher temperature as it remains in contact with the wall for longer duration.

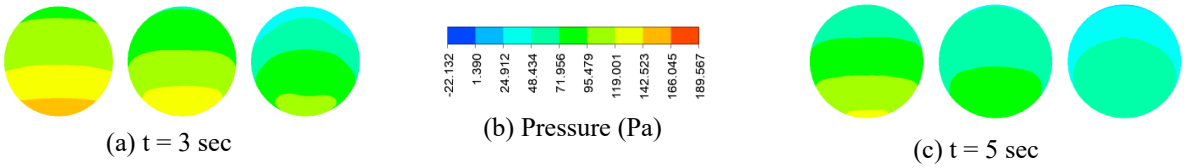

(a) t = 3 sec (b) Pressure (Pa) (c) t = 5 sec

Figure 4.45: Pressure contours ($G = 20.08\ kg/m^2.s$)
Plane1 (left) - Plane3 (right)

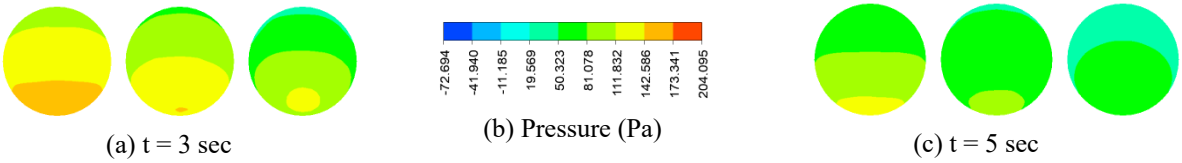

(a) t = 3 sec (b) Pressure (Pa) (c) t = 5 sec

Figure 4.46: Pressure contours ($G = 66.9\ kg/m^2.s$)
Plane1 (left) - Plane3 (right)

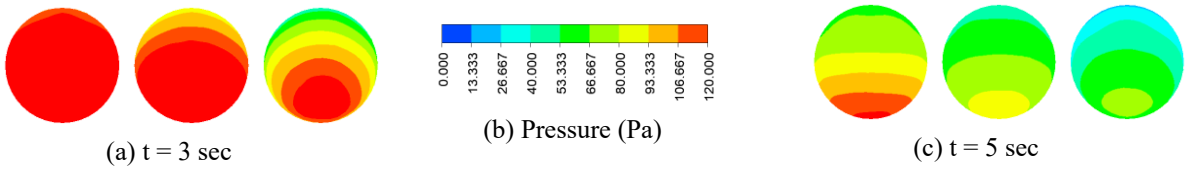

(a) t = 3 sec (b) Pressure (Pa) (c) t = 5 sec

Figure 4.47: Pressure contours ($G = 133.8\ kg/m^2.s$)
Plane1 (left) - Plane3 (right)

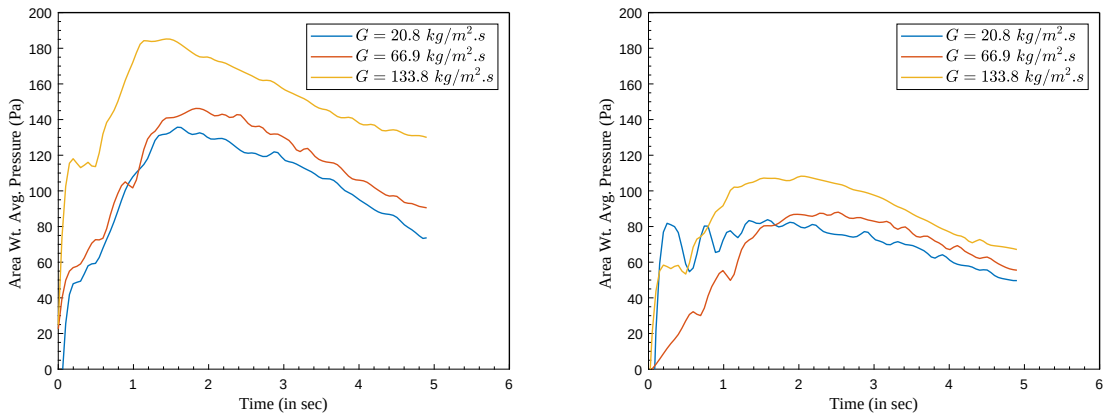

(a) Plane 1 (b) Plane 3

Figure 4.48: Pressure distribution for different mass flux

The total pressure variation during the phenomena is represented in Figure4.48.A pressure rise in the line is observed when phase change takes place. As the expansion ratio during phase change is very high this leads to surge in pressure and velocity readings which can be seen from Figure 4.52.Figure 4.45,4.46 , 4.47 depicts the pressure at three planes at different times and different mass flux.There is a pressure drop in the line as time progresses.

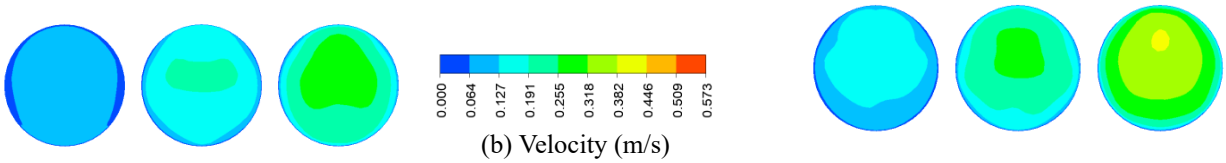

(a) t = 3 sec (b) Velocity (m/s) (c) t = 5sec

Figure 4.49: Velocity contours ($G = 20.08\ kg/m^2.s$)
Plane1 (left) - Plane3 (right)

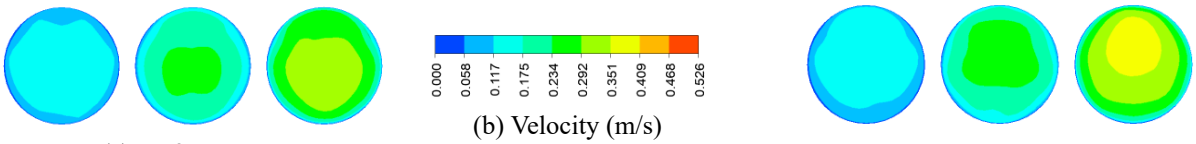

(a) t = 3 sec (b) Velocity (m/s) (c) t = 5sec

Figure 4.50: Velocity contours ($G = 66.9\ kg/m^2.s$)
Plane1 (left) - Plane3 (right)

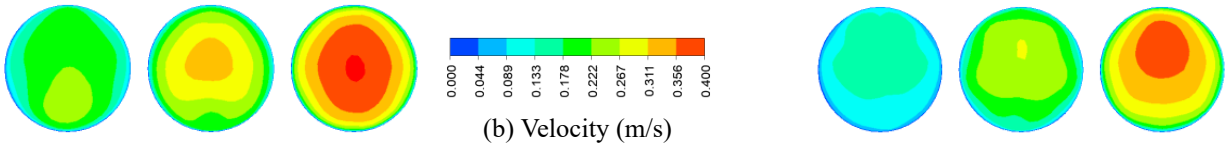

(a) t = 3 sec (b) Velocity (m/s) (c) t = 5sec

Figure 4.51: Velocity contours ($G = 133.8\ kg/m^2.s$)
Plane1 (left) - Plane3 (right)

As vapor reaches the top sections and adhere to the walls, high velocities are observed. The cryogen that flows towards downstream sections have larger surface area for heat transfer and hence accumulate into gaseous form with high velocity undergoing phase change.Also with increase in mass flux , the average velocity at a section increases just as depicted in 4.52.

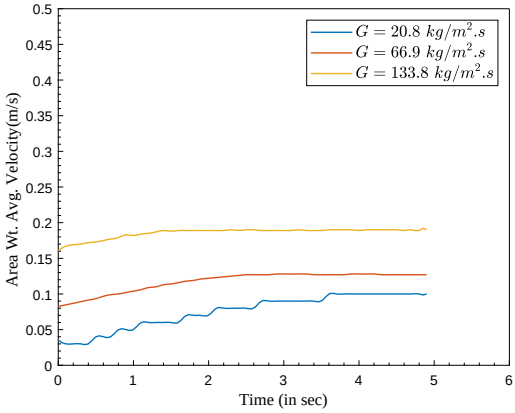

(a) Plane 1

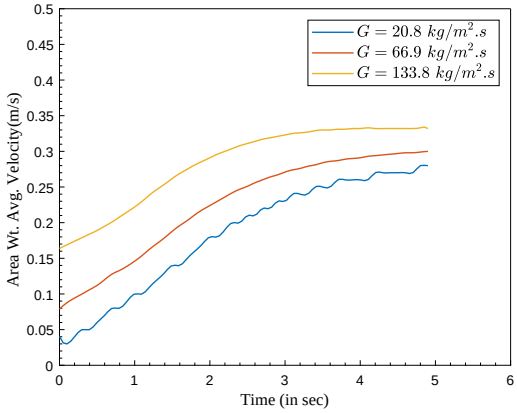

(b) Plane 3

Figure 4.52: Velocity distribution for different mass flux

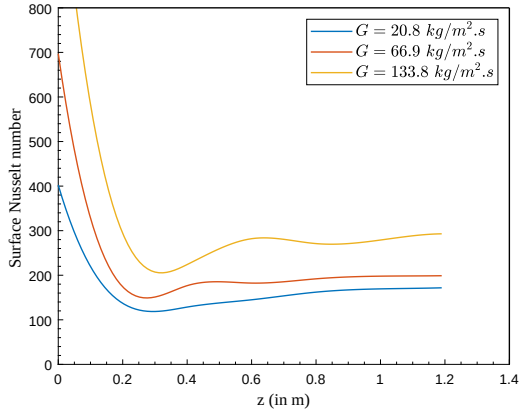

(a) t = 1 sec

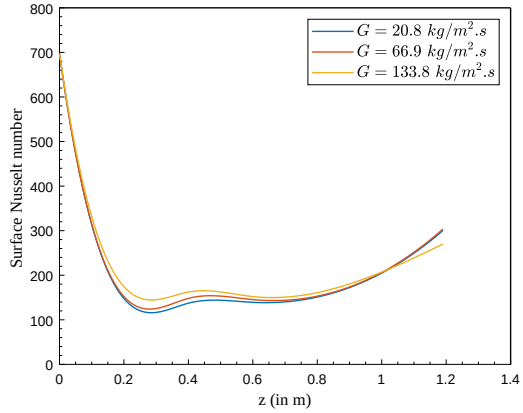

(b) t = 5 sec

Figure 4.53: Nusselt number along the length for different mass flux

Figure 4.53 shows the variation of Nusselt number along the length of transfer line. At t=1 sec , the presence of vapor is very less. With increasing mass flux the heat transfer coefficient increases which and there is a marginal upward slope at the downstream indicating the effect of low thermal conductive vapor presence.It is seen that reduction in thermal conductivity is much larger than the drop in heat transfer coefficient.At t=5sec, convection completely dominates the heat transfer as presence of gaseous nitrogen impedes heat transfer through conduction. However, it is seen that the heat transfer rates and coefficients had similar values for different mass flux.

Chapter 5

Conclusion

Chilldown phenomena is an initial transient process that each and every cryogenic system must experience before reaching its intended operation.A transfer line, in its basic form, is an uninsulated pipeline that handles and transfers cryogenic fluid.

Chilldown of a transfer line involves two phase flow with different patterns originating from the thermal interactions between cold fluid and hot wall.Film boiling regime is responsible for most of the wall chilldown.

From the simulations performed in the present work, it was found that integrating phase change with multiphase flow in ANSYS FLUENT requires a good understanding of modeling equations and its applicability to current scenario.
Some of the important deductions from the work are pointed below:

- The transfer line is assumed to be filled with liquid cryogen at 77K with surrounding wall at 300K.As a result, there is a large heat flux into the system resulting in formation of gaseous nitrogen.
- During the phase change process, pressure surges are seen in the line. With increasing mass flux, these pressure surges increase as well.
- The expansion ratio of nitrogen is 1:696. When liquid phase absorbs required latent heat and changes its phase, gaseous phase starts expanding, thereby converting the pressure energy into kinetic energy.Hence local velocities are much higher than the inlet velocity.
- As mass flux is varied from low to high,velocity at any arbitrary plane increases.
- Because of its lower density, GN_2 accumulates at top of the line leaving LN_2 to flow beneath,thereby showing a stratified two phase flow pattern.
- The vapor distribution contours showed that when high mass flux are prevalent at inlet, the liquid cryogen had the ability to quickly reach the downstream planes.
- At low mass flux, the line is predominantly filled with GN_2 since the incoming cryogen quickly boiled off at upstream itself.

- At low mass flux the presence of GN_2 for most of the time greatly impedes the heat transfer rate and low wall heat fluxes are encountered.This also has a considerable effect on chilldown time.
- With increase in mass flux, the wall cooled down much quicker owing to effective advection taking place at higher flow rates.
- The presence of pronounced stratified pattern lead to a circumferential distribution of temperature of the wall.However this was only specific of higher mass flux ($> 133.8kg/m^2.s$). At low mass flux, this distribution doesn't occur due to the absence of two phase flow, mostly at the downstream.
- The presence of two phase flow at higher mass flux greatly influences the heat transfer rates occurring at upstream and downstream.With time, the accumulation of vapor on top of the line, results in lower heat transfer rate especially at downstream sections.
- When a constant heat flux is persistent to the transfer line that is already near cryogenic temperature,it still lead to formation of vapor bubbles that adhered o the walls.
- The fluid temperature at any particular plane decreases with increasing mass flux as more amount of liquid cryogen balanced out the super-heated gaseous nitrogen.
- The downstream sections showed similar presence of vapor at considered mass fluxes.
- Modeling phase change with Lee Evaporation-Condensation model requires evaluating coefficients that decide the mass transfer rate. There is no definitive theoretical method that is prescribed for a particular flow phenomena.Instead, it has been reported by many authors that these coefficients change depending upon the boiling and bubble dynamics. These values can only be found out by rigorous experimentation.

Two phase flow regimes haven't been clearly identified in the present work. Film boiling is considered to be the existing regime taking into account the pool boiling curve. Modeling nucleate boiling requires information about bubble growth and its dynamics. The material properties of transfer line is an important consideration at low temperatures since the thermal stability and structural integrity should not be compromised while handling cryogenic fluids. These studies can be a major area of research.

5.1 Scope for further research

While the common understanding of chilldown phenomena is straight forward, science involved within is extremely complicated.Two phase flow regimes during chilldown are

not clearly defined and are vastly dependent on experimental conditions.Therefore a large conglomeration of data sets is required which can only be enabled by extensive research.

ANSYS FLUENT is a robust tool for fluid flow simulations. However modeling boiling and two phase flow has certain limitations.Multiphase models available in FLUENT are specific to flow patterns. In problems like cryogenic chilldown, where multiple flow regimes exist both spatially and temporally, no single multiphase flow model can be applied to simulate whole chilldown process. Hence, the solver methods have to be modified depending upon the problem. This requires the knowledge of coding with external software packages.These limitations would encourage employing other numerical tools which perform better.

In present work, the computational capabilities were a major constraint. The Volume Of Fluid model is one of the simpler approaches to multiphase flow modeling.The problem scenario which consisted separate initial conditions to fluid and solid domain renders it to be a demonstrative approach towards chilldown. Other Euler-Euler approaches present in FLUENT can be explored as well. Incorporating conditions to shift boiling regimes as per available wall superheat is another area which can be explored in the numerical front.Evaluating heat transfer coefficients which dynamically change during each boiling regime cannot be computed by default FLUENT software. The correlations that are analytically available in context of cryogenic flow boiling are dependent on hydrodynamic flow behavior and other related dimensionless parameters. Implementing these relations into CFD code to simulate a full scale chilldown phenomena is worth being explored.

Chilldown phenomena of other transfer lines carrying other cryogenic fluids like LH_2, LO_2 can be investigated. The boiling regimes that occur during this phenomena can be compared. For instance, LH_2 line chilldown does not explicitly show the presence of distinct boiling regimes. Optimal angle for faster chilldown of a transfer line is one such study where the effect of inclination on chilldown times is explored. A chilldown strategy for longer transfer lines can be further developed to reduce the loss of cryogen in boil off.

Cryogenic systems are being employed in deep space exploration for many years now. In-Situ Resource Utilization proposed by NASA aims at using space resources to generate breathable air,cryogenic liquid propellant in future.Operational capabilities of these systems is an important aspect and chilldown,which is greatly affected by gravity plays a vital role.

References

[1] Burke, J., Byrnes, W., Post, A. & Ruccia, F. Pressurized cooldown of cryogenic transfer lines. In *Advances in Cryogenic Engineering*, 378–394 (Springer, 1960).

[2] Chato, D. & Sanabria, R. Review and test of chilldown methods for space-based cryogenic tanks. In *27th Joint Propulsion Conference*, 1843 (1991).

[3] LeClair, A. & Majumdar, A. Computational model of the chilldown and propellant loading of the space shuttle external tank. In *46th AIAA/ASME/SAE/ASEE Joint Propulsion Conference & Exhibit*, 6561 (2010).

[4] Srinivasan, K., Rao, V. S. & Murthy, M. K. Analytical and experimental investigation on cool-down of short cryogenic transfer lines. *Cryogenics* **14**, 489–494 (1974).

[5] Krishnamurthy, M., Chandra, R., Jacob, S., Kasthurirengan, S. & Karunanithi, R. Experimental studies on cool-down and mass flow characteristics of a demountable liquid nitrogen transfer line. *Cryogenics* **36**, 435–441 (1996).

[6] Burggraf, O. An exact solution of the inverse problem in heat conduction theory and applications (1964).

[7] Wang, J. *et al.* Transient modeling of cryogenic two-phase flow boiling during chill-down process. *Applied Thermal Engineering* **143**, 461–471 (2018).

[8] Darr, S. *et al.* An experimental study on terrestrial cryogenic transfer line chilldown i. effect of mass flux, equilibrium quality, and inlet subcooling. *International Journal of Heat and Mass Transfer* **103**, 1225–1242 (2016).

[9] Jin, L., Park, C., Cho, H., Lee, C. & Jeong, S. Experimental investigation on chill-down process of cryogenic flow line. *Cryogenics* **79**, 96–105 (2016).

[10] Shaeffer, R., Hu, H. & Chung, J. An experimental study on liquid nitrogen pipe chilldown and heat transfer with pulse flows. *International Journal of Heat and Mass Transfer* **67**, 955–966 (2013).

[11] Hartwig, J., Styborski, J., McQuillen, J., Rame, E. & Chung, J. Liquid hydrogen line chilldown experiments at high reynolds numbers. optimal chilldown methods. *International Journal of Heat and Mass Transfer* **137**, 703–713 (2019).

[12] Hartwig, J. *et al.* Liquid hydrogen line chilldown experiments at high reynolds numbers. ii. analysis. *International Journal of Heat and Mass Transfer* **156**, 119805 (2020).

[13] Johnson, J. & Shine, S. Transient cryogenic chill down process in horizontal and inclined pipes. *Cryogenics* **71**, 7–17 (2015).

[14] Shukla, A., Sridharan, A. & Atrey, M. Investigation of transient chill down phenomena in tubes using liquid nitrogen. In *IOP Conference Series: Materials Science and Engineering*, vol. 278, 012035 (IOP Publishing, 2017).

[15] Cross, M., Bennett, J., Majumdar, A. & Malla, R. Modeling of chill down in cryogenic transfer lines. *Journal of Spacecraft and Rockets - J SPACECRAFT ROCKET* **39**, 284–289 (2002).

[16] Miropolskiy, Z. Heat transfer in film boiling of a steam-water mixture in steam-generator tubes. *Teplonergetika* **10**, 49–52 (1963).

[17] Darr, S. R. *et al.* Numerical simulation of the liquid nitrogen chilldown of a vertical tube. In *53rd aiaa aerospace sciences meeting*, 0468 (2015).

[18] Chen, J., Zeng, R., Chen, H. & Xie, J. Effects of wall superheat and mass flux on flow film boiling in cryogenic chilldown process. *AIP Advances* **10**, 015123 (2020).

[19] Agarwal, A. *Numerical simulation of cryogenic flow with phase change using sharp interface cut-cell method* (University of Florida, 2010).

[20] Das Chaudhury, M. & Ghosh, S. Numerical inspection of chilldown process in cryogenic transportation line (2019).

[21] Darr, S. *et al.* The effect of reduced gravity on cryogenic nitrogen boiling and pipe chilldown. *npj Microgravity* **2**, 1–9 (2016).

[22] Kawanami, O., Azuma, H. & Ohta, H. Effect of gravity on cryogenic boiling heat transfer during tube quenching. *International journal of heat and mass transfer* **50**, 3490–3497 (2007).

[23] Antar, B. Flow boiling during quench in low gravity environment. *Int. J. Microgravity Research and Appl.* **3**, 118–128 (1997).

[24] Yuan, K., Ji, Y., Chung, J. & Shyy, W. Cryogenic boiling and two-phase flow during pipe chilldown in earth and reduced gravity. *Journal of Low Temperature Physics* **150**, 101 (2008).

[25] Guide, A. F. T. Ansys fleunt teory guide (2013).

[26] Marquardt, E., Le, J. & Radebaugh, R. Cryogenic material properties database. In *Cryocoolers 11*, 681–687 (Springer, 2002).

[27] Yunus, A. C. *Fluid Mechanics: Fundamentals And Applications (Si Units).* (Tata McGraw Hill Education Private Limited, 2010).

[28] Carbajo, J. J. A study on the rewetting temperature. *Nuclear Engineering and Design* **84**, 21–52 (1985). URL `https://www.sciencedirect.com/science/article/pii/0029549385903103`.

[29] De Salve, M. & Panella, B. 4.12 analytical model for bottom reflooding thermal-hydraulics in circular ducts and comparison with experimental results. In *Advanced Course in Heat Transfer in Nuclear Reactor Safety* (Begel House Inc., 1980).